

1 **The Sal-like 4 - integrin $\alpha 6\beta 1$ network promotes cell migration for metastasis via**
2 **activation of focal adhesion dynamics in basal-like breast cancer cells.**

3

4 Junji Itou^{1*}, Sunao Tanaka¹, Wenzhao Li¹, Atsuo Iida², Atsuko Sehara-Fujisawa²,
5 Fumiaki Sato¹, Masakazu Toi¹

6

7 1. Department of Breast Surgery, Graduate School of Medicine, Kyoto University, 54
8 Shogoin-Kawahara-cho, Sakyo-ku, Kyoto 606-8507, Japan

9 2. Department of Growth Regulation, Institute of Frontier Medical Sciences, Kyoto
10 University, 53 Shogoin-Kawahara-cho, Sakyo-ku, Kyoto 606-8397, Japan

11

12 *Corresponding author:

13 Junji Itou

14 54 Shogoin-Kawahara-cho, Sakyo-ku, Kyoto 606-8507, Japan

15 Tel: +81-75-751-3660, Fax: +81-75-751-3616

16 e-mail: junji-itou@umin.ac.jp

17 **Abstract**

18 During metastasis, cancer cell migration is enhanced. However, the mechanisms
19 underlying this process remain elusive. Here, we addressed this issue by functionally
20 analyzing the transcription factor Sal-like 4 (SALL4) in basal-like breast cancer cells.
21 Loss-of-function studies of SALL4 showed that this transcription factor is required for
22 the spindle-shaped morphology and the enhanced migration of cancer cells. SALL4 also
23 up-regulated integrin gene expression. The impaired cell migration observed in SALL4
24 knockdown cells was restored by overexpression of integrin $\alpha 6$ and $\beta 1$. In addition, we
25 clarified that integrin $\alpha 6$ and $\beta 1$ formed a heterodimer. At the molecular level, loss of
26 the SALL4 - integrin $\alpha 6\beta 1$ network lost focal adhesion dynamics, which impairs cell
27 migration. Over-activation of Rho is known to inhibit focal adhesion dynamics. We
28 observed that SALL4 knockdown cells exhibited over-activation of Rho. Aberrant Rho
29 activation was suppressed by integrin $\alpha 6\beta 1$ expression, and pharmacological inhibition
30 of Rho activity restored cell migration in SALL4 knockdown cells. These results
31 indicated that the SALL4 - integrin $\alpha 6\beta 1$ network promotes cell migration via
32 modulation of Rho activity. Moreover, our zebrafish metastasis assays demonstrated

33 that this gene network enhances cell migration *in vivo*. Our findings identify a potential
34 new therapeutic target for the prevention of metastasis, and provide an improved
35 understanding of cancer cell migration.

36

37 **Highlights**

38 SALL4 up-regulates integrin $\alpha6\beta1$ expression at the transcription level.

39 The SALL4 - integrin $\alpha6\beta1$ network is required for a spindle-shaped morphology.

40 The SALL4 - integrin $\alpha6\beta1$ network activates focal adhesion dynamics.

41 The SALL4 - integrin $\alpha6\beta1$ network modulates Rho activation for cell migration.

42

43 **Keywords**

44 Breast cancer; Cell migration; Focal adhesion dynamics; Integrin; SALL4

45

46 **Abbreviations**

47 ECM: extracellular matrix, FA: Focal adhesion, FAK: Focal adhesion kinase, SALL4:

48 Sal-like 4

49 **1. Introduction**

50 In contrast to normal cells, cancer cells display metastatic properties, including
51 migration, invasion and anoikis resistance. During metastasis, cells must migrate to
52 depart from the primary site and travel to other tissues and organs. However, little is
53 known about how cancer cells change their character to enhance migratory properties.
54 Knowledge of the underlying mechanism may help prevent metastasis, and will
55 contribute to the understanding of cancer cells.

56 Transcription factors control cellular characteristics through the regulation of
57 gene expression. Sal-like 4 (SALL4) is a zinc finger transcription factor. SALL4 has
58 two isoforms, SALL4A and SALL4B [1, 2]; the SALL4A transcript includes the entire
59 exon 2, while SALL4B has a truncated version. In breast cancer cells, SALL4 is
60 positively regulated by signal transduction and activator of transcription 3 [3]. In breast
61 cancer patients, SALL4 levels were shown to be increased in the circulating tumor cells
62 [4]. A positive correlation between SALL4 expression and lymph node metastasis has
63 been reported in colorectal cancer patients [5, 6]. In addition to these clinical
64 observations, our previous study showed that loss of SALL4 function reduced cell

65 motility in cell lines of basal-like breast cancer, which is the most aggressive and
66 metastatic subtype among breast cancers [7]. Therefore SALL4 appears to be involved
67 in cancer cell migration. However, the role of SALL4 in migration has not been fully
68 elucidated.

69 Basal-like breast cancer is known to be an aggressive breast cancer subtypes.
70 This cancer seems to originate from normal mammary cells that have epithelial gene
71 expression and low migratory properties. However, in contrast to normal cells,
72 basal-like breast cancer cells express mesenchymal genes, and possess high migratory
73 properties. Thus, using basal-like breast cancer cell lines allowed us to analyze the
74 acquisition of a high migratory ability. In 2-dimensional cultures, the cells are dispersed,
75 and exhibit a polarized, spindle-shaped morphology.

76 A number of molecules have been shown to be involved in the polarized cell
77 migration. Integrin is a cell-extracellular matrix (ECM) adhesion protein, and is known
78 to promote migration [8]. The integrin α subunit and β subunit form a heterodimer on
79 the cell membrane with an extracellular domain that binds ECM molecules [9, 10]. In

80 the human genome, there are 18 α and 8 β subunit genes. Ligand specificities are
81 different in each heterodimer, for example, integrin $\alpha6\beta1$ binds to laminin-511 [11].

82 In the inside of a cell, focal adhesion (FA) is organized where integrins form a
83 cluster [12, 13]. FA generates actin cytoskeleton, and activation of intracellular
84 signaling pathways [8, 12]. FA complex contains proteins involved in cytoskeleton
85 anchoring, such as paxillin, vinculin and talin, and in intracellular signaling, such as
86 focal adhesion kinase (FAK). During FA maturation, FAK is phosphorylated at Tyr-397,
87 and activates downstream signaling to promote migration [14, 15].

88 For cell migration, the FA assembly/disassembly cycle must be active.
89 Therefore, in addition to FA formation and maturation, FA turn over is required [16, 17].
90 FAK is one of the factors for FA turn over [8]. To disassemble FA, FAK signaling
91 inhibits the activity of the Rho GTPase that stabilizes FA [18, 19]. Rho inhibition by
92 FAK results in enhancement of FA dynamics and cell migration.

93 In this study, we investigated the role of SALL4 in cell migration. We
94 demonstrated morphological change of the cells from spindle-shaped to rounded and the
95 loss of migration following SALL4 knockdown in basal-like breast cancer cells. We

96 found that SALL4 positively regulates the integrin $\alpha 6$ and $\beta 1$ genes. Rescue
97 experiments with integrin $\alpha 6$ and $\beta 1$ showed restoration of cell morphology and the
98 migratory properties in SALL4 knockdown cells. Moreover, we discovered that the
99 SALL4 - integrin $\alpha 6\beta 1$ network mediates FAK activation and Rho inhibition to
100 promote cell migration in basal-like breast cancer. Our zebrafish metastasis assays
101 revealed that the SALL4 - integrin $\alpha 6\beta 1$ network also enhances migration *in vivo*. This
102 study proposes a novel mechanism of how basal-like breast cancer cells acquire high
103 migratory properties.

104

105 **2. Material and Methods**

106 *2.1 Cell culture*

107 SUM159 cells were obtained from Astrerand (Detroit, MI, USA), and maintained with
108 Ham's F-12 nutrient mixture containing 5% FBS, 5 $\mu\text{g}/\text{mL}$ insulin, 1 $\mu\text{g}/\text{mL}$
109 hydrocortisone and 10 mM HEPES. MDA-MB-231 cells were obtained from the
110 American Type Culture Collection (Manassas, VA, USA), and maintained with
111 RPMI-1640 containing 10% FBS. For drug selection to obtained infectants, 1 $\mu\text{g}/\text{mL}$

112 puromycin, 10 µg/mL blasticidin S or 250 µg/mL hygromycin B was used. Images of
113 cultured cells were collected with an all-in-one microscope, BZ-9000 (Keyence, Osaka,
114 Japan). Cell growth was analyzed as previously described [20].

115

116 *2.2 Loss- and gain-of-function studies*

117 For gene knockdown, a lentivector, pLKO (Addgene, 8453, Cambridge, MA, USA),
118 was used. Double-strand DNA with shRNA sequence was inserted into the region
119 between *EcoRI* and *AgeI* sites of the pLKO vector. The shRNA target sequences are
120 listed in Supplementary Table S1. For the gene overexpression experiments, a pLenti
121 vector (Life Technologies, V533-06, Carlsbad, CA, USA) was used. The EF1 α
122 promoter sequence was amplified from the pEF1 α -mCherry-N1 vector (Takara, 631969,
123 Kusatsu, Japan), and inserted between the *ClaI* and *SpeI* sites. The gene coding region
124 was cloned into a pENTR-FLAG vector [20], and subsequently subcloned into the
125 pLenti vector with the EF1 α promoter.

126 Lentiviral particles were produced as described previously [7]. Lenti-X 293T cells
127 (Takara, 632180) were used. In loss-of-function studies, infected cells were analyzed 6
128 days after infection.

129

130 *2.3 Boyden chamber assays*

131 Cells were suspended in serum-free medium, placed into the upper component of the
132 chamber at a density of 400 cells/mm², and incubated for 1h at 37 °C. Then, medium
133 containing 5% serum was added to the lower component. After 5h of incubation at
134 37 °C, the cells were fixed with 4% paraformaldehyde in PBS for 15 min, and washed
135 with PBS. Cells at the upper side were wiped out. Migrated cells were stained with
136 Hoechst 33342 (Dojindo, 346-07951, Kamimashiki, Japan, 1:500 dilution). The number
137 of migrated cells was analyzed in a 300 mm² region in the central area of a chamber.
138 The cells were counted manually.

139

140 *2.4 Immunostaining*

141 Cells were plated on a glass bottom chamber slide (Matsunami glass, SCS-008, Osaka,
142 Japan), and cultured for 2 days. To suppress the activity of Rho signaling, the cells were
143 treated with 1 $\mu\text{g}/\text{mL}$ C3 transferase (Cytoskeleton, CT04, Denver, CO, USA) for 2h, or
144 10 μM Y-27632 (Wako, 257-00511, Osaka, Japan) for 4h. Half of the medium was
145 removed, and an equal amount of 4% paraformaldehyde in PBS was added (final
146 concentration was 2%) for fixation. Cells were fixed for 15-20 min at room temperature,
147 and washed with PBS containing 0.05% Tween 20. Permeabilization was performed
148 with 0.5% Triton X-100 in PBS for 15 min at room temperature. The blocking solution
149 contained 5% goat serum and 1% BSA in PBS. The primary antibodies were
150 anti-phospho-paxillin antibody (Cell Signaling Technology, 2541, Danvers, MA, USA,
151 1:20 dilution), anti-GM130 antibody (Cell Signaling Technology, 12480, 1:3200
152 dilution), anti-integrin $\alpha 6$ antibody (Acris Antibodies GmbH, Herford, Germany, 1:100
153 dilution) and anti-integrin $\beta 1$ antibody (GeneTex, GTX23167, Alton Pkwy Irvine, CA,
154 USA, 1:10 dilution). The Secondary antibodies were goat anti-mouse IgG antibody
155 conjugated to Alexa Fluor 647 (Life Technologies, A21235, 1/1000 dilution), goat
156 anti-rat IgG antibody conjugated to Alexa Fluor 488 (Cell Signaling Technology, 4416,

157 1/1000 dilution) and goat anti-rabbit IgG antibody conjugated to Alexa Fluor 488 (Life
158 Technologies, A11008, 1/1000 dilution). Hoechst 33342 was used for nuclear staining.
159 Images of immunostained samples were collected with a BZ-9000 microscope
160 (Keyence). Optical sections were obtained with a confocal platform, TCS SP8 (Leica,
161 Tokyo, Japan).

162

163 *2.5 Messenger RNA expression analyses*

164 Total RNA samples were extracted with TRIzol reagent (Life Technologies, 15596026).
165 The RNA-seq analysis was previously described [20]. Complementary DNA samples
166 were synthesized from 1 µg of total RNA with SuperScript III (Life Technologies,
167 18080044), and quantitative reverse transcription-polymerase chain reaction
168 (qRT-PCR) was performed with a reagent, FastStart Universal SYBR Green Master
169 (Roche, 04913850001, Mannheim, Germany). Primers for qRT-PCR are listed in
170 Supplementary Table S2.

171

172 *2.6 Promoter activity analyses*

173 The SALL4A and SALL4B coding regions were cloned downstream of the CAG
174 promoter obtained from pCAG-mGFP (Addgene, 14757). To assess the promoter
175 activities, 1kbp regions upstream of the transcription start sites of the *ITGA6* and *ITGB1*
176 genes were linked to the minimal promoter in the pGL4.30 vector that also carries a
177 firefly luciferase2 gene (Promega, E8481, Madison, WI, USA). The promoter reporter
178 was co-transfected into Lenti-X 293T cells with the pGL4.73 vector that has the SV40
179 promoter and a Renilla luciferase gene (Promega, E6911), and with the SALL4
180 expression vector. A transfection reagent, FuGENE HD (Promega, E2311) was used.
181 One day after transfection, luciferase activity was measured using the Dual-Glo
182 Luciferase Assay System (Promega, E2920).

183

184 *2.7 Chromatin immunoprecipitation*

185 The SALL4B coding sequence was cloned into the pENTR-FLAG vector, and
186 subsequently subcloned into the pLenti vector. Cells expressing FLAG or
187 SALL4B-FLAG were cultured and used for chromatin immunoprecipitation. The
188 procedure was performed as previously described [20], and an anti-FLAG M2 antibody

189 (Sigma, F1804, St. Louis, MO, USA) was used. Immunoprecipitated DNA fragments
190 were used for regular PCR. The primers for *ITGA6* promoter were as follows: forward
191 5'-GCATCACCTGCACTTCTCTTTAT-3' and reverse
192 5'-CTGTGGACAGAATTGTGGTTG-3'. The primers for *ITGB1* promoter were as
193 follows: forward 5'-GGAGTCGCGGAACAGCAG-3' and reverse
194 5'-CCGGCGGCTTTAAGTGCT-3'. PCR products were electrophoresed with a 6%
195 acrylamide gel.

196

197 *2.8 Immunoblotting*

198 The primary antibodies were anti-phospho-FAK antibody (Cell Signaling Technology,
199 8556, 1:1000 dilution), anti-FAK antibody (Cell Signaling Technology, 3285, 1:1000
200 dilution), and anti-integrin β 1 antibody (Cell Signaling Technology, 9699, 1:1000
201 dilution). Detection of the immunoreactions was described previously [20]. The
202 intensity of each band was analyzed using ImageJ.

203 For analysis of phosphorylated FAK levels, cells were starved with medium
204 containing 0.5% FBS for 18 h. Then, cells were trypsinized and suspended with

205 medium containing 0.1% BSA. The suspended cells were incubated for 1 h at 37 °C.
206 Cells were then plated onto a TC-coated culture dish. After a 1 h incubation, cells were
207 harvested for analyses.

208 To obtain immunoprecipitated samples of integrin $\alpha 6$ complex,
209 co-immunoprecipitation was performed with approximately 0.5 g of cells. A Dynabeads
210 Co-Immunoprecipitation Kit (Veritas, DB14321, Tokyo, Japan) and the anti-FLAG M2
211 antibody were used. Additionally, 0.5% NP-40 was added to the extraction buffer from
212 the kit.

213 Rho signals were detected with rabbit anti-RhoA antibody (Cell Signaling
214 Technology, 8789, 1:667 dilution). RhoA activity was measured with RhoA G-LISA
215 Activation Assay Kit (Cytoskeleton, BK124).

216

217 *2.9 Laminin binding assay*

218 For the laminin binding assays, 400 μ L of PBS containing 1 μ g of recombinant
219 laminin-511 E8 fragment (Nippi, 892013, Tokyo, Japan) was added to the wells of a
220 24-well plate and incubated for 1 h at 37 °C. The wells were washed, blocked with 1%

221 BSA solution for 1 h at 37 °C, and washed again. Then, 10,000 cells were plated, and
222 incubated for 20 min at 37 °C. The wells were washed, and the number of bound cells
223 was analyzed. The cells were counted manually.

224

225 *2.10 Time-lapse imaging*

226 The EGFP gene was cloned into the pENTR-FLAG vector. The paxillin coding
227 sequence was inserted the *NcoI* site of the pENTR-EGFP-FLAG vector. The
228 paxillin-EGFP fusion construct was subcloned into the pLenti vector (Life Technologies,
229 V533-06). Cells labeled with paxillin-EGFP were plated on a TC-coated glass bottom
230 dish (Greiner, 627975, Frickenhausen, Germany). Time-lapse images were collected
231 using a BZ-9000 microscope with a CO₂ chamber (Keyence).

232

233 *2.11 Transplantation assays*

234 For mouse xenograft assay, 1 x 10⁵ MDA-MB-231 cells were suspended in 80 uL of
235 serum-free medium with 50% Matrigel (Corning, 356237, Bedford, MA, USA), and
236 transplanted into the mammary fat pad of five-week-old nude mouse. In the same

237 mouse, shGFP (control) and shSALL4 cells were injected at the right and the left sides,
238 respectively.

239 For zebrafish metastasis assay, cancer cell lines were labeled with mCherry
240 via lentiviral infection. Two-day-old *fli1-EGFP* fish embryos were dechorionated and
241 embedded into 1.0% low-melt agarose. Approximately 30 cells were injected into the
242 abdominal cavity. Transplanted embryos were maintained at 32 °C for 3 days, and
243 observed with a BZ-9000 microscope (Keyence).

244 The animal experiments in this study were approved by the Ethics Review
245 Board for Animal Experiments of Kyoto University. All animals were maintained
246 according to the Guide for the Care and Use of Laboratory Animals (National Institute
247 of Health Publication).

248

249 *2.12 Statistical analyses*

250 The number of migrated cell, the ratio of the FA-rich region, mRNA levels, luciferase
251 activity, phosphorylated FAK levels, the cell number bound to the laminin-511 E8
252 fragment, the active Rho level, and cell growth were analyzed using Student's *t*-test.

253 The ratio of polarized cells and the metastasis rate in the zebrafish assay were analyzed
254 using Fisher's exact test. For TCGA data, *SALL4* expression levels among breast cancer
255 subtypes were analyzed using a Kruskal-Wallis H test, and *ITGA6* and *ITGB1*
256 expression levels were analyzed using a Mann-Whitney *U* test. $P < 0.05$ was considered
257 statistically significant.

258

259 **3. Results**

260 *3.1 SALL4 is required for cell migration and normal FA pattern.*

261 To investigate the role of *SALL4* in cell migration, we conducted loss-of-function
262 studies. We used a previously established shRNA system that targets the common
263 sequence of the *SALL4* isoforms (sh*SALL4*) [7]. shRNA for the GFP gene (shGFP)
264 was used as a control. We introduced shRNA expression into basal-like breast cancer
265 cell lines, SUM159 and MDA-MB-231, which are both highly migratory, and have a
266 spindle-shaped morphology. We found that the *SALL4* knockdown cells were rounded,
267 while there was no morphological change in the shGFP control cells (Fig. 1A). Because
268 rounded morphology is indicative of low migratory potential, we explored changes in

269 the migratory properties of SALL4 knockdown cells. Using Boyden chamber assays,
270 we observed a loss of migration following SALL4 knockdown in SUM159 and
271 MDA-MB-231 cells (Fig. 1B,C), indicating that SALL4 positively regulates cell
272 migration.

273 In a polarized migrating cell, FAs are observed in restricted areas of the cell
274 periphery, whereas a low migratory cell has expanded FA-rich peripheral regions [21,
275 22]. To analyze the FA pattern, we immunostained cells with an antibody for
276 phosphorylated paxillin, which is a marker of FAs. In the control cells, FAs were
277 localized to the restricted areas, while the FA-positive area was expanded in SALL4
278 knockdown cells (Fig. 1D). To quantify this difference, we measured the length of the
279 FA-rich region, and divided it by the perimeter (Supplementary Fig. S1). In SALL4
280 knockdown cells, the ratio of the FA-rich region to the perimeter was significantly
281 increased (Fig. 1E). This result indicates that SALL4 modulates the FA pattern, which
282 may result in a spindle-shaped morphology and the high migratory properties.

283 A migrating cell has front-rear polarity, and loss of polarity results in a
284 rounded morphology and reduction in migration. Therefore SALL4 knockdown cells

285 may have lost this polarity. GM130 is a Golgi marker, and the Golgi apparatus is
286 localized near the front of the nucleus in a polarized cell. If the polarity is lost, the
287 GM130 signal is observed around the nucleus. We analyzed GM130 signals, and
288 observed no difference in the percentages of polarized cells between the controls and
289 SALL4 knockdown cells (Fig. 1F,G). This result suggests that SALL4 is not involved in
290 the regulation of cell polarity.

291

292 *3.2 SALL4 up-regulates integrin genes.*

293 Since SALL4 is a transcription factor, we hypothesized that it regulates the expression
294 of genes involved in cell migration. To identify SALL4-regulated genes, we obtained
295 gene expression data by RNA-seq, and compared the data from the shGFP and
296 shSALL4 groups (deposited in the DNA Data Bank of Japan, Sequence Read Archive
297 as DRA004721 and DRA004722, respectively) (Fig. 2A, [Supplementary Table S3](#)). We
298 found that the expression of several integrin genes was reduced by SALL4 knockdown.
299 Because integrin is known to promote cell migration, we focused on integrin family
300 genes. To validate the result of RNA-seq analysis, we performed qRT-PCR (Fig. 2B).

301 We identified candidate genes, namely *ITGA3*, *ITGA6*, *ITGA10*, *ITGB1* and *ITGB4*, the
302 expression levels of which were reduced to less than half of that of the controls by
303 SALL4 knockdown in both SUM159 and MDA-MB-231 cells.

304 To determine which integrin gene is involved in basal-like breast cancer cell
305 migration under the control of SALL4, we performed shRNA-mediated knockdown for
306 each gene. Morphological analysis showed that knockdowns of integrin $\alpha 6$ (encoded by
307 *ITGA6*) and $\beta 1$ (encoded by *ITGB1*) induced a rounded morphology, similar to the
308 SALL4 knockdown (Fig. 2C), while the others showed no notable changes
309 (Supplementary Fig. S2). Next, we analyzed the migratory properties of these cells, and
310 observed significant reductions in migration (Fig. 2D). Although knockdown of each
311 candidate gene impaired cell migration, only the integrin $\alpha 6$ and $\beta 1$ knockdowns
312 reduced the migration to levels similar to that of SALL4 knockdown (Fig. 2D). These
313 results suggest that reduced expression of integrin $\alpha 6$ and $\beta 1$ is involved in the rounded
314 morphology and the reduced migration of SALL4 knockdown cells.

315 To study the regulation of integrin $\alpha 6$ and $\beta 1$ expression by SALL4, we
316 performed reporter assays with the promoter regions of the *ITGA6* and *ITGB1* genes.

317 We linked each promoter region to the minimal promoter (miniP) and the luciferase2
318 reporter gene. We then prepared expression vectors carrying each SALL4 isoform.
319 Co-transfection with the integrin promoter reporter and the SALL4 expression vector
320 resulted in up-regulation of reporter gene expression, while no increase was observed in
321 the miniP control (Fig. 2E), indicating that both SALL4 isoforms activate the promoters
322 of the *ITGA6* and *ITGB1* genes. To determine whether SALL4 binds to these promoters,
323 we introduced FLAG-tagged SALL4B expression vectors to MDA-MB-231 cells, and
324 performed chromatin immunoprecipitation assays with an anti-FLAG M2 antibody. The
325 results showed an enrichment of the *ITGA6* and *ITGB1* promoter regions in the sample
326 of SALL4B-FLAG cells (Fig. 2F). These observations suggest that SALL4 directly
327 up-regulates integrin $\alpha 6$ and $\beta 1$ at the transcriptional level.

328 The Cancer Genome Atlas (TCGA) network has published the gene
329 expression data of a number of cancer patients [23]. We analyzed the expression levels
330 of SALL4 in breast cancer patients, and found that it was up-regulated in the cancer
331 tissues of basal-like breast cancer patients (Supplementary Fig. S3A). To assess the
332 correlation with integrin gene expression, we classified the basal-like breast cancer

333 patients to two groups, SALL4 high and SALL4 low. The SALL4 high group had
334 higher SALL4 expression in the cancer tissues than in the normal tissues of the same
335 patient. We observed higher integrin $\alpha 6$ and $\beta 1$ expression in the SALL4 high group
336 than in the SALL4 low group (Supplementary Fig. S3B). These results suggest that
337 SALL4 up-regulates integrin $\alpha 6$ and $\beta 1$ expression in basal-like breast cancer.

338

339 *3.3 SALL4-regulated integrin $\alpha 6$ and $\beta 1$ promote migration.*

340 To determine whether SALL4 promotes cell migration via up-regulation of integrin $\alpha 6$
341 and $\beta 1$, we performed rescue experiments by overexpressing integrin $\alpha 6$ and $\beta 1$ in
342 SALL4 knockdown cells. We constructed overexpression vectors for the integrin $\alpha 6$
343 variants, $\alpha 6v1$ and $\alpha 6v2$ (also known as $\alpha 6B$ and $\alpha 6A$, respectively), and $\beta 1$
344 (Supplementary Fig. S4A). The two transcriptional variants of integrin $\alpha 6$ share an
345 extracellular domain and a transmembrane region, but have different cytoplasmic tails
346 [24]. We introduced these expression vectors into MDA-MB-231 cells, and obtained
347 stably expressing cells (Supplementary Fig. S4B). The results of the migration assays
348 showed that cell migration was restored when the cells overexpressed both integrin $\alpha 6$

349 and $\beta 1$, but integrin $\alpha 6$ alone and $\beta 1$ alone were not able to rescue the migratory ability
350 of SALL4 knockdown cells (Fig. 3A). In addition to cell migration, the rounded
351 morphology caused by SALL4 knockdown was restored in the cells overexpressing
352 both integrin $\alpha 6$ and $\beta 1$ (Fig. 3B). These results indicate that SALL4-regulated integrin
353 $\alpha 6$ and $\beta 1$ are required for the spindle-shaped morphology and cell migration in
354 basal-like breast cancer cells.

355 Because integrin mediates FAs, we analyzed the FA pattern. In SALL4
356 knockdown cells, the FA-positive area was expanded compared to that of the control,
357 but this change was not observed in the cells overexpressing integrin $\alpha 6$ and $\beta 1$ (Fig.
358 3C). Additionally, the FA-rich region was significantly expanded by SALL4
359 knockdown, and no change was observed in the cells overexpressing integrin $\alpha 6$ and $\beta 1$
360 (Fig. 3D).

361 In integrin-mediated FAs, FAK is phosphorylated at Tyr-397 [14]. We
362 analyzed the levels of phosphorylated FAK in the cells overexpressing integrin $\alpha 6$ and
363 $\beta 1$ (Fig. 3E). In the control cells, reduced FAK phosphorylation was observed following
364 SALL4 knockdown (Fig. 3F). However, overexpression of both integrin $\alpha 6$ and $\beta 1$

365 restored the phosphorylated FAK levels (Fig. 3F), suggesting that integrin $\alpha 6$ and $\beta 1$
366 are required for FAK activation. Our observations indicate that SALL4 modulates FAs
367 via up-regulation of integrin $\alpha 6$ and $\beta 1$.

368

369 *3.4 Integrin $\alpha 6$ and $\beta 1$ form a heterodimer in basal-like breast cancer.*

370 The integrin α and β subunits form a heterodimer [9, 10]. Integrin $\alpha 6$ and $\beta 1$ can bind
371 to each other [25], but it is unclear whether they form a heterodimer in basal-like breast
372 cancer cells. To clarify this, we conducted a co-immunoprecipitation assay in
373 MDA-MB-231 cells. We precipitated protein complexes from the lysates of cells
374 overexpressing FLAG-tagged integrin $\alpha 6$ using an anti-FLAG M2 antibody. We
375 detected integrin $\beta 1$ in the protein complexes of integrin $\alpha 6 v 1$ and $\alpha 6 v 2$ (Fig. 4A),
376 indicating that integrin $\alpha 6$ and $\beta 1$ form a heterodimer. Furthermore, we
377 double-immunostained SUM159 and MDA-MB-231 cells with antibodies for integrin
378 $\alpha 6$ and $\beta 1$, and performed optical sectioning with a confocal microscope (Fig. 4B). We
379 observed overlapping signals, supporting that there are integrin $\alpha 6 \beta 1$ heterodimers in
380 basal-like breast cancer cells.

381 The integrin $\alpha6\beta1$ heterodimer can bind to laminin-511 [11]. Because SALL4
382 up-regulates integrin $\alpha6$ and $\beta1$ expression, and integrin $\alpha6$ and $\beta1$ form a heterodimer,
383 we hypothesized that SALL4 knockdown cells lose the ability to bind to laminin-511. If
384 integrin $\alpha6$ and $\beta1$ do not form a heterodimer in basal-like breast cancer cells, there will
385 be no change in the laminin-511 binding ability in SALL4 knockdown cells. To address
386 this hypothesis, we performed a binding assay with a recombinant laminin-511 E8
387 fragment to which integrin binds [26]. We used a BSA solution for blocking. A small
388 number of cells bound to the BSA-coated dish, and there was no difference in the
389 number of bound cells between the control and SALL4 knockdown cells (Fig. 4C).
390 When we coated a dish with the laminin-511 E8 fragment in combination with the BSA
391 blocking solution, the number of bound SUM159 and MDA-MB-231 cells increased.
392 Additionally, we observed that the number of bound SALL4 knockdown cells was
393 approximately half that of the controls (Fig. 4D), indicating that SALL4 promotes the
394 binding to laminin-511. Furthermore, we performed rescue experiments by
395 overexpressing integrin $\alpha6$ and $\beta1$, and the binding to laminin-511 was restored (Fig.

396 4E,F). These results showed that the SALL4-regulated integrin $\alpha 6$ and $\beta 1$ function by
397 forming an $\alpha 6\beta 1$ heterodimer.

398

399 *3.5 SALL4 is required for FA dynamics.*

400 Impaired FA assembly/disassembly dynamics causes changes in the FA pattern and loss
401 of migration. To analyze the FA dynamics, we monitored the localization of paxillin, a
402 component of the FA complex, using a paxillin-EGFP fusion construct. We obtained
403 images at 0 and 10 min, and observed the FA assembly/disassembly (Fig. 5A). FA
404 signals appeared as punctate dots, while the free paxillin-EGFP molecules localized
405 near the nucleus and appeared as diffuse signals. In these experiments, we used an
406 shRNA with a scrambled sequence (shScr) as the control. In the control cells, assembled
407 and disassembled FAs were observed (Fig. 5A, arrowheads). However, FAs in SALL4
408 knockdown cells were unchanged, suggesting that FAs were stabilized by SALL4
409 knockdown.

410 We quantified the ratios of assembled and disassembled FAs in each cell (Fig.
411 5B,C). The ratio of assembled FAs was calculated by dividing the number of newly

412 formed FAs in 10 min by the total number of FAs at 10 min. The ratio of disassembled
413 FAs was calculated by dividing the number FAs lost in 10 min by the total number of
414 FAs at 0 min. The results showed that both the ratios of assembled and disassembled
415 FAs were reduced by SALL4 knockdown, and this reduction was restored by
416 overexpression of integrin $\alpha6\beta1$, suggesting that FA stabilization in SALL4 knockdown
417 cells is due to the loss of integrin $\alpha6\beta1$. These observations indicate that the SALL4 -
418 integrin $\alpha6\beta1$ network activates the FA dynamics.

419

420 *3.6 The SALL4 - integrin $\alpha6\beta1$ network prevents aberrant Rho activation in cell*
421 *migration.*

422 Loss of FAK causes over-activation of Rho [18]. Rho over-activation stabilizes FAs,
423 and reduces cell migration [8, 22, 27]. In the SALL4 knockdown cells, FAK
424 phosphorylation levels and migration were reduced, and these reductions were restored
425 by integrin $\alpha6\beta1$ expression (Fig. 3). We therefore hypothesized that the SALL4 -
426 integrin $\alpha6\beta1$ network is involved in regulating Rho activity in cell migration. Thus, we
427 measured Rho activity, and observed that SALL4 knockdown did not change the

428 protein level of Rho, but increased RhoA activity (Fig. 6A,B). In SALL4 knockdown
429 cells, Rho over-activation was suppressed by integrin $\alpha6\beta1$ (Fig. 6B). These results
430 indicate that the SALL4 - integrin $\alpha6\beta1$ network prevents Rho over-activation in
431 basal-like breast cancer cells.

432 To determine whether over-activation of Rho is the responsible for the
433 rounded morphology and expansion of the FA-rich region in SALL4 knockdown cells,
434 we treated SALL4 knockdown cells with Rho signaling inhibitors, C3 transferase and
435 Y-27632. C3 transferase ADP-ribosylates Asn-41 on the Rho family of small GTPases,
436 Rho A, B and C [28]. We analyzed cell morphology following C3 transferase treatment
437 in SALL4 knockdown cells, and observed that the treated cells exhibited a
438 spindle-shaped morphology and a reduced FA-rich region (Supplementary Fig. S5).
439 Rho A activates Rho-associated coiled-coil forming protein serine/threonine kinase
440 (ROCK). Appropriate activation and suppression of the Rho-ROCK pathway is required
441 for cell migration [8, 22, 27]. We used a chemical ROCK inhibitor, Y-27632 [29], and
442 observed that the rounded morphology of the SALL4 knockdown cells converted to a
443 spindle-shaped morphology (Fig. 6C). In addition, expansion of the FA-rich region was

444 not observed in Y-27632-treated cells (Fig. 6D). These results indicate that SALL4
445 regulates cell morphology and the FA pattern through modulation of Rho activity.

446 Long-term treatment with C3 transferase causes cellular stress, and increases
447 the difficulty in analyzing cell migration. Y-27632 is milder than C3 transferase in
448 basal-like breast cancer cells, and it is easier to assess cell migration following Y-27632
449 treatment. Using Boyden chamber assays, we analyzed the number of cells that
450 migrated in 5 hours, and found that the reduced cell migration was recovered by ROCK
451 inhibition in SALL4 knockdown cells (Fig. 6E). Taken together, the SALL4 - integrin
452 $\alpha6\beta1$ network promotes cell migration through modulation of the Rho-ROCK pathway
453 (Supplementary Fig. S6).

454

455 *3.7 The SALL4 - integrin $\alpha6\beta1$ network is required for in vivo cell migration.*

456 SALL4 knockdown reduces cell growth [7, 30], and the reduced cell growth was not
457 rescued by integrin $\alpha6\beta1$ expression (Supplementary Fig. S7A). This indicates that the
458 mouse transplantation model can not be used to analyze the *in vivo* migratory properties
459 of SALL4 knockdown cells, because the tumor size of the SALL4 knockdown cells can

460 not be compared to that of the controls at both the transplanted focus and the metastatic
461 foci, and evaluation using the number of foci and/or the size of metastatic tumors is not
462 accurately show a difference in migration. In support of this notion, our mouse
463 xenograft experiments showed the reduced tumor growth in SALL4 knockdown cells
464 (Supplementary Fig. S7B). Therefore, to analyze *in vivo* cell migration, we used
465 zebrafish metastasis assays. These assays require 2 or 3 days to assess migration, and do
466 not require cell growth and tumor formation [31].

467 We labeled basal-like breast cancer cells with a red fluorescent protein,
468 mCherry, and the cells were transplanted to the abdominal cavity of 2-day-old embryos
469 of *fli1-EGFP* fish that expressed green fluorescent protein in the vascular endothelial
470 cells [32]. When we transplanted metastatic cancer cells, they moved into the blood
471 vessels, subsequently migrated out to other organs, such as the brain and trunk. We
472 monitored the migration of transplanted cells and observed metastasis (Fig. 7A).
473 Circulating cancer cells were observed as overlapping signals of EGFP and mCherry.
474 Metastasized cells were observed as separate signals (Fig. 7A, arrowheads). Most fish

475 with control cancers underwent metastasis, while few fish with SALL4 knockdown
476 cells showed metastasis.

477 During the zebrafish metastasis assay, we noted that several cancer cells
478 circulated from end to end of the body in the blood stream in a few seconds, which
479 suggested that analysis of migratory distance is inadequate to analyze the migratory
480 properties. Therefore we analyzed the metastatic rate using methods from previous
481 studies [31, 33]. We counted the number of fish with or without metastasis, and
482 calculated the ratio of fish with metastasis (Fig. 7B). The results showed that the
483 metastatic rate was significantly reduced by SALL4 knockdown, indicating that SALL4
484 positively regulates the migratory ability *in vivo* as well as *in vitro*.

485 We next determined whether integrin $\alpha6\beta1$ expression restores *in vivo*
486 migration in SALL4 knockdown cells. We transplanted cells overexpressing integrin
487 $\alpha6\beta1$ and observed similar migration rates as that of the controls in SALL4 knockdown
488 cells (Fig. 7C). These results indicate that the SALL4 - integrin $\alpha6\beta1$ network is
489 required for enhanced migration *in vivo*.

490

491 *3.8 Integrin $\alpha6\beta1$ expression is an indicator of poor metastasis-free survival.*

492 The integrin $\alpha6\beta1$ -regulated cell migration suggests that integrin $\alpha6\beta1$ expression
493 promotes metastasis in breast cancer patients. To investigate the relationship between
494 integrin $\alpha6\beta1$ expression and metastasis, we analyzed publically available clinical data
495 using the SurvExpress platform [34]. Six clinical studies from five cohorts have
496 published data on mRNA expression and metastasis-free survival [35-39]. The data
497 from three studies showed that the breast cancer patients with high integrin $\alpha6\beta1$
498 expression had a lower metastasis-free survival rate than that of the patients with low
499 integrin $\alpha6\beta1$ expression (Supplementary Fig. S8A-C). However, data from the other 3
500 studies showed no significant difference between the integrin $\alpha6\beta1$ high and low groups
501 (Supplementary Fig. S8D-F). These results suggest that integrin $\alpha6\beta1$ expression may
502 promote metastasis in some cases.

503

504 **4. Discussion**

505 One of the crucial steps in cancer metastasis is the acquisition of the high migratory
506 properties. In this study, we elucidated the role of the SALL4 - integrin $\alpha6\beta1$ network

507 in cell migration in basal-like breast cancer cells. SALL4 knockdown cells showed
508 reduced migration and a rounded morphology with expansion of the FA-rich region.
509 Gene expression analyses revealed that SALL4 positively regulates the expression of
510 the integrin $\alpha 6$ and $\beta 1$ genes. Cells with loss of integrin $\alpha 6$ and $\beta 1$ showed identical
511 phenotypes to that of SALL4 knockdown cells, suggesting that they are the causative
512 factors of SALL4-regulated cell migration. Overexpression of both integrin $\alpha 6$ and $\beta 1$
513 restored cell migration and reversed the morphology in SALL4 knockdown cells,
514 further supporting this notion. Moreover, we observed that SALL4 knockdown cells
515 have aberrant Rho activation, and integrin $\alpha 6\beta 1$ expression suppressed this phenotype.
516 Pharmacological inhibition of Rho over-activation restored cell migration in SALL4
517 knockdown cells. These results suggest that the SALL4 - integrin $\alpha 6\beta 1$ network is
518 required for cell migration via modulation of Rho activity. In addition, we performed
519 zebrafish metastasis assays, and showed that exogenous integrin $\alpha 6\beta 1$ expression
520 restored cell migration in SALL4 knockdown cells, indicating that the SALL4 - integrin
521 $\alpha 6\beta 1$ network promotes cell migration *in vivo*. Our findings identify a novel mechanism
522 underlying the high migratory properties of cancer cells.

523 SALL4 is known to be a factor in stem cell maintenance and proliferation [2,
524 40]. In cancer cells, SALL4 up-regulates genes involved in cell proliferation, such as
525 *BMI1* and *CCND1* [7, 41, 42]. However, the role of SALL4 in cell migration has not
526 been fully elucidated, because SALL4-depleted cells display impaired cell proliferation,
527 which hinders the analysis of other biological features. In this study, we used an
528 shRNA-mediated SALL4 knockdown system, and prepared fresh SALL4 knockdown
529 cells in each experiment. We performed SALL4 loss-of-function studies in the
530 basal-like breast cancer cell lines, SUM159 and MDA-MB-231. The cells have a
531 spindle-shaped morphology and high migratory properties, and these characteristics can
532 be altered by genetic manipulation and pharmacological treatment, which allowed us to
533 easily analyze the role of SALL4 in cell migration. Using this procedure, we elucidated
534 the role of SALL4 in cell migration.

535 Although our previous study found that SALL4 is involved in the
536 spindle-shaped morphology of basal-like breast cancer cells [7], the causative factors
537 and the detailed mechanism underlying this characteristic remained elusive. In this
538 study, we discovered that the SALL4 - integrin $\alpha6\beta1$ network regulates the

539 spindle-shaped morphology through the maintenance of FA dynamics. We observed an
540 expansion of the FA-rich region in SALL4 knockdown cells. However, SALL4
541 knockdown cells did not show a reduction in FA number, although SALL4 knockdown
542 reduces the mRNA levels of several integrin genes. No reduction in FA number may be
543 due to the function of the remaining integrins. SALL4 knockdown reduced expression
544 levels of its downstream genes, including integrins, but it did not completely deplete
545 their expression. In addition, cells express other integrins that are not regulated by
546 SALL4. Therefore SALL4 knockdown cells had reduced integrin function, which
547 appeared to be sufficient to form FAs, but not for activation of FA dynamics.

548 Although knockdown of each SALL4-regulated integrin gene showed reduced
549 cell migration, this study focused on the integrin $\alpha 6$ and $\beta 1$ genes, because the
550 morphological change and the degree of reduction in the migration following their
551 knockdowns were identical to those of the SALL4 knockdown. The integrin $\alpha 6\beta 1$
552 heterodimer was found to be the main factor in SALL4-regulated cell migration. The
553 human genome has 18 integrin α and 8 integrin β subunit genes, and various integrin
554 genes are expressed in basal-like breast cancer. Although integrins appear to be

555 involved in cancer metastasis, the role of each integrin has not been fully characterized
556 in metastatic process, such as cell migration, invasion, and anoikis resistance. In this
557 study, through analyses of SALL4 function, we showed that integrin $\alpha6\beta1$ is required
558 for migration during basal-like breast cancer metastasis. Additionally, analyses of the
559 data from several cohort studies showed that breast cancer patients with high integrin
560 $\alpha6$ and $\beta1$ expression had poorer metastasis-free survival than that of the patients with
561 low integrin $\alpha6$ and $\beta1$ expression. These results suggest that a therapy targeting
562 integrin $\alpha6\beta1$ will inhibit metastasis by suppressing cell migration.

563 Integrin $\alpha6$ has two variants. The functions of the integrin $\alpha6$ variants differ
564 with respect to stemness [43, 44]. However, we observed that the variants have
565 comparable role in cell migration. Integrin $\beta1$ cytoplasmic tail binds to FAK to form
566 focal adhesion, and to activate FAK signaling for cell migration [45]. Because the
567 integrin $\alpha6$ extracellular and transmembrane domains are shared by the variants, and
568 overexpression of each variant restored the reduced cell migration of SALL4
569 knockdown cells in combination with integrin $\beta1$ overexpression, integrin $\alpha6$ may
570 function to support integrin $\beta1$ in SALL4-regulated cell migration.

571 In SALL4 knockdown cells, the FAs were stabilized, and the FA dynamics
572 were restored by inhibition of Rho signaling. Aberrant Rho activity was normalized by
573 exogenous expression of integrin $\alpha6\beta1$. We thought that the SALL4 - integrin $\alpha6\beta1$
574 network modulates Rho activity to promote cell migration. Although Rho activation is
575 required for FA maturation, its over-activation stabilizes FA, which in turn inhibits the
576 FA assembly/disassembly cycle. Our results showed that the SALL4 - integrin $\alpha6\beta1$
577 network modulates Rho activity, but we did not identify the Rho activation factor.
578 There are a number of factors involved in Rho activation [19], and they might function
579 in FA maturation in basal-like breast cancer cells.

580 This study showed that the SALL4 up-regulates integrin signaling, and
581 modulates Rho activity. However there is a possibility that SALL4 regulates genes
582 involved in recruitment of FA molecules, such as *PAG3* (paxillin-associated protein
583 with ADP-rebosylation factor [ARF] GTPase-activating protein [GAP] activity, number
584 3) (also known as ASAP2/KIAA0400) [46]. *PAG3* recruits paxillin molecules to FA,
585 and *PAG3* overexpression impairs cell migration in leukemic monocyte lymphoma cell
586 line, U937, and kidney cell line, COS-7 [46]. We therefore analyzed the relation

587 between SALL4 and PAG3. However, in our RNA-seq analysis, SALL4 does not
588 regulate *PAG3* expression. We did not observed enrichment of *PAG3* upstream region
589 in ChIP assay. In our unpublished observation, although the morphology of basal-like
590 breast cancer cells overexpressing PAG3 was slightly rounded, it is still spindle-shaped.
591 These suggest that PAG3 is not involved in the function of SALL4 with respect to cell
592 migration.

593 In addition to cell migration, integrins are involved in cell growth [47].
594 However, overexpression of integrin $\alpha6\beta1$ did not restore the cell growth in SALL4
595 knockdown cells, implying that integrin $\alpha6\beta1$ is not involved in SALL4-regulated cell
596 growth. Due to the impaired cell growth of SALL4 knockdown cells, we are not able to
597 compare tumor sizes at the transplanted focus and metastatic foci between control and
598 SALL4 knockdown cells in mouse transplantation assay. Therefore, instead of mouse
599 transplantation assays, we utilized zebrafish metastasis assays that allowed us to analyze
600 the migration of single cells in 2-3 days without cell growth [31]. In the zebrafish assay,
601 we observed reduced cell migration in SALL4 knockdown cells, and restoration of
602 migration by integrin $\alpha6\beta1$ expression, consistent with the results of the *in vitro*

603 experiments. Our results demonstrated that the zebrafish metastasis assay is a useful
604 tool to analyze cell migration *in vivo*, especially if cells show reduced growth. Although
605 the conditions, such as temperature, osmotic pressure and nutrients, are different
606 between human and zebrafish bodies, and the results do not strictly reflect the cancer
607 cell behavior in the human body, we can use zebrafish to evaluate the *in vivo* migration
608 potential.

609 A correlation between SALL4 expression and cancer metastasis has been
610 reported in colorectal cancer [5, 6]. Circulating tumor cells have high SALL4 levels in
611 breast cancer patients [4]. However, it was unclear how SALL4 promotes metastasis.
612 This study bridges the gap between observations of SALL4 expression and metastasis.
613 In addition, we identified integrin $\alpha 6\beta 1$ as a causative factor of SALL4-regulated cell
614 migration. This study contributes to elucidating cancer cell migration, and suggests a
615 therapeutic target to prevent metastasis. SALL4 is expressed in various cancers [48]. An
616 anti-SALL4 peptide prevents tumor growth in a mouse transplantation model, and may
617 be useful as a treatment for liver cancer [49]. Our findings suggest the possibility of
618 SALL4-targeted therapies for metastasis.

619

620 **5. Conclusions**

621 This study discovered the SALL4 - integrin $\alpha6\beta1$ network in metastatic cancer cells.

622 Our data contributes to understanding of the regulation of metastasis. Although several

623 factors are involved in metastasis, and the SALL4 - integrin $\alpha6\beta1$ network is not likely

624 to be activated in all metastatic cancers, this study may contribute to a future therapy for

625 breast cancer patients with high SALL4 expression.

626

627 **Conflict of interest**

628 JI is an employee of Kyoto University's Sponsored Research Program funded by Taiho

629 Pharmaceutical Co., Ltd. ST, WL, AI, ASF and FS received no specific funding for this

630 work. MT received research funding from Taiho Pharmaceutical Co., Ltd. The funding

631 sources had no role in the study design, experiment, analysis, interpretation or writing

632 the manuscript. The corresponding author had full access to the data and final

633 responsibility for submission.

634

635 **Acknowledgements**

636 We thank Dr Kojiro Taura for sharing the time-lapse imaging system. We thank the
637 members of departments of breast surgery, and of hepato-biliary-pancreatic surgery and
638 transplantation for sharing laboratory equipment. We thank the Medical Research
639 Support Center, Graduate School of Medicine, Kyoto University for technical assistance.
640 RNA-seq was performed by Eurofins Genomics Japan. Financial supports were
641 provided by Taiho Pharmaceutical Co., Ltd., and by The Ichiro Kanehara Foundation
642 No. 15KI275.

643

644 **Appendices**

645 Supplementary materials

646 **Supplementary Table S3**

647

648 **References**

649 [1] Y. Ma, W. Cui, J. Yang, J. Qu, C. Di, H.M. Amin, R. Lai, J. Ritz, D.S.
650 Krause, L. Chai, SALL4, a novel oncogene, is constitutively expressed in
651 human acute myeloid leukemia (AML) and induces AML in transgenic mice,
652 Blood, 108 (2006) 2726-2735.

653 [2] S. Rao, S. Zhen, S. Roumiantsev, L.T. McDonald, G.C. Yuan, S.H. Orkin,
654 Differential roles of Sall4 isoforms in embryonic stem cell pluripotency,
655 *Molecular and cellular biology*, 30 (2010) 5364-5380.

656 [3] J.D. Bard, P. Gelebart, H.M. Amin, L.C. Young, Y. Ma, R. Lai, Signal
657 transducer and activator of transcription 3 is a transcriptional factor
658 regulating the gene expression of SALL4, *FASEB journal : official*
659 *publication of the Federation of American Societies for Experimental Biology*,
660 23 (2009) 1405-1414.

661 [4] C. Panis, L. Pizzatti, A.C. Herrera, R. Cecchini, E. Abdelhay, Putative
662 circulating markers of the early and advanced stages of breast cancer
663 identified by high-resolution label-free proteomics, *Cancer letters*, 330 (2013)
664 57-66.

665 [5] M.M. Forghanifard, M. Moghbeli, R. Raeisossadati, A. Tavassoli, A.J.
666 Mallak, S. Boroumand-Noughabi, M.R. Abbaszadegan, Role of SALL4 in the
667 progression and metastasis of colorectal cancer, *Journal of biomedical*
668 *science*, 20 (2013) 6.

669 [6] L. Hao, Y. Zhao, Z. Wang, H. Yin, X. Zhang, T. He, S. Song, S. Sun, B.
670 Wang, Z. Li, Q. Su, Expression and clinical significance of SALL4 and
671 beta-catenin in colorectal cancer, *Journal of molecular histology*, 47 (2016)
672 117-128.

673 [7] J. Itou, Y. Matsumoto, K. Yoshikawa, M. Toi, Sal-like 4 (SALL4)
674 suppresses CDH1 expression and maintains cell dispersion in basal-like
675 breast cancer, *FEBS letters*, 587 (2013) 3115-3121.

676 [8] A. Huttenlocher, A.R. Horwitz, Integrins in cell migration, *Cold Spring*
677 *Harbor perspectives in biology*, 3 (2011) a005074.

678 [9] S.J. Shattil, C. Kim, M.H. Ginsberg, The final steps of integrin activation:
679 the end game, *Nature reviews. Molecular cell biology*, 11 (2010) 288-300.

680 [10] I.D. Campbell, M.J. Humphries, Integrin structure, activation, and
681 interactions, *Cold Spring Harbor perspectives in biology*, 3 (2011).

682 [11] R. Nishiuchi, J. Takagi, M. Hayashi, H. Ido, Y. Yagi, N. Sanzen, T. Tsuji,
683 M. Yamada, K. Sekiguchi, Ligand-binding specificities of laminin-binding
684 integrins: a comprehensive survey of laminin-integrin interactions using
685 recombinant alpha3beta1, alpha6beta1, alpha7beta1 and alpha6beta4

686 integrins, *Matrix biology : journal of the International Society for Matrix*
687 *Biology*, 25 (2006) 189-197.

688 [12] M.A. Wozniak, K. Modzelewska, L. Kwong, P.J. Keely, Focal adhesion
689 regulation of cell behavior, *Biochimica et biophysica acta*, 1692 (2004)
690 103-119.

691 [13] C. Albiges-Rizo, O. Destaing, B. Fourcade, E. Planus, M.R. Block, Actin
692 machinery and mechanosensitivity in invadopodia, podosomes and focal
693 adhesions, *Journal of cell science*, 122 (2009) 3037-3049.

694 [14] A. Hamadi, M. Bouali, M. Dontenwill, H. Stoeckel, K. Takeda, P. Rondé,
695 Regulation of focal adhesion dynamics and disassembly by phosphorylation
696 of FAK at tyrosine 397, *Journal of cell science*, 118 (2005) 4415-4425.

697 [15] G.W. McLean, N.O. Carragher, E. Avizienyte, J. Evans, V.G. Brunton,
698 M.C. Frame, The role of focal-adhesion kinase in cancer - a new therapeutic
699 opportunity, *Nature reviews. Cancer*, 5 (2005) 505-515.

700 [16] S. Stehbens, T. Wittmann, Targeting and transport: how microtubules
701 control focal adhesion dynamics, *The Journal of cell biology*, 198 (2012)
702 481-489.

703 [17] M. Nagano, D. Hoshino, N. Koshikawa, T. Akizawa, M. Seiki, Turnover
704 of focal adhesions and cancer cell migration, *International journal of cell*
705 *biology*, 2012 (2012) 310616.

706 [18] X.D. Ren, W.B. Kiosses, D.J. Sieg, C.A. Otey, D.D. Schlaepfer, M.A.
707 Schwartz, Focal adhesion kinase suppresses Rho activity to promote focal
708 adhesion turnover, *Journal of cell science*, 113 (Pt 20) (2000) 3673-3678.

709 [19] S. Huveneers, E.H. Danen, Adhesion signaling - crosstalk between
710 integrins, Src and Rho, *Journal of cell science*, 122 (2009) 1059-1069.

711 [20] W. Li, J. Itou, S. Tanaka, T. Nishimura, F. Sato, M. Toi, A homeobox
712 protein, NKX6.1, up-regulates interleukin-6 expression for cell growth in
713 basal-like breast cancer cells, *Experimental cell research*, 343 (2016)
714 177-189.

715 [21] D.J. Sieg, C.R. Hauck, D.D. Schlaepfer, Required role of focal adhesion
716 kinase (FAK) for integrin-stimulated cell migration, *Journal of cell science*,
717 112 (Pt 16) (1999) 2677-2691.

718 [22] L.M. McHardy, K. Warabi, R.J. Andersen, C.D. Roskelley, M. Roberge,
719 Strongylophorine-26, a Rho-dependent inhibitor of tumor cell invasion that
720 reduces actin stress fibers and induces nonpolarized lamellipodial extensions,
721 *Molecular cancer therapeutics*, 4 (2005) 772-778.

722 [23] TCGA, Comprehensive molecular portraits of human breast tumours,
723 *Nature*, 490 (2012) 61-70.

724 [24] R.N. Tamura, H.M. Cooper, G. Collo, V. Quaranta, Cell type-specific
725 integrin variants with alternative alpha chain cytoplasmic domains,
726 *Proceedings of the National Academy of Sciences of the United States of*
727 *America*, 88 (1991) 10183-10187.

728 [25] C. Klockenbusch, J. Kast, Optimization of formaldehyde cross-linking
729 for protein interaction analysis of non-tagged integrin beta1, *Journal of*
730 *biomedicine & biotechnology*, 2010 (2010) 927585.

731 [26] T. Miyazaki, S. Futaki, H. Suemori, Y. Taniguchi, M. Yamada, M.
732 Kawasaki, M. Hayashi, H. Kumagai, N. Nakatsuji, K. Sekiguchi, E. Kawase,
733 Laminin E8 fragments support efficient adhesion and expansion of
734 dissociated human pluripotent stem cells, *Nature communications*, 3 (2012)
735 1236.

736 [27] A.J. Ridley, RhoA, RhoB and RhoC have different roles in cancer cell
737 migration, *Journal of microscopy*, 251 (2013) 242-249.

738 [28] K. Aktories, C. Wilde, M. Vogelsgesang, Rho-modifying C3-like
739 ADP-ribosyltransferases, *Reviews of physiology, biochemistry and*
740 *pharmacology*, 152 (2004) 1-22.

741 [29] M. Uehata, T. Ishizaki, H. Satoh, T. Ono, T. Kawahara, T. Morishita, H.
742 Tamakawa, K. Yamagami, J. Inui, M. Maekawa, S. Narumiya, Calcium
743 sensitization of smooth muscle mediated by a Rho-associated protein kinase
744 in hypertension, *Nature*, 389 (1997) 990-994.

745 [30] D. Kobayashi, K. Kuribayashi, M. Tanaka, N. Watanabe, SALL4 is
746 essential for cancer cell proliferation and is overexpressed at early clinical
747 stages in breast cancer, *International journal of oncology*, 38 (2011) 933-939.

748 [31] Y. Teng, X. Xie, S. Walker, D.T. White, J.S. Mumm, J.K. Cowell,
749 Evaluating human cancer cell metastasis in zebrafish, *BMC cancer*, 13
750 (2013) 453.

751 [32] N.D. Lawson, B.M. Weinstein, In vivo imaging of embryonic vascular
752 development using transgenic zebrafish, *Developmental biology*, 248 (2002)
753 307-318.

754 [33] C. Thomas, G. Rajapaksa, F. Nikolos, R. Hao, A. Katchy, C.W.
755 McCollum, M. Bondesson, P. Quinlan, A. Thompson, S. Krishnamurthy, F.J.
756 Esteva, J. Gustafsson, ERbeta1 represses basal breast cancer epithelial to
757 mesenchymal transition by destabilizing EGFR, *Breast cancer research :*
758 *BCR*, 14 (2012) R148.

759 [34] R. Aguirre-Gamboa, H. Gomez-Rueda, E. Martínez-Ledesma, A.
760 Martínez-Torteya, R. Chacolla-Huaranga, A. Rodriguez-Barrientos, J.G.
761 Tamez-Peña, V. Treviño, SurvExpress: an online biomarker validation tool
762 and database for cancer gene expression data using survival analysis, *PloS*
763 *one*, 8 (2013) e74250.

764 [35] K. Chin, S. DeVries, J. Fridlyand, P.T. Spellman, R. Roydasgupta, W.L.
765 Kuo, A. Lapuk, R.M. Neve, Z. Qian, T. Ryder, F. Chen, H. Feiler, T.
766 Tokuyasu, C. Kingsley, S. Dairkee, Z. Meng, K. Chew, D. Pinkel, A. Jain,
767 B.M. Ljung, L. Esserman, D.G. Albertson, F.M. Waldman, J.W. Gray,
768 Genomic and transcriptional aberrations linked to breast cancer
769 pathophysiologies, *Cancer cell*, 10 (2006) 529-541.

770 [36] K.J. Kao, K.M. Chang, H.C. Hsu, A.T. Huang, Correlation of
771 microarray-based breast cancer molecular subtypes and clinical outcomes:
772 implications for treatment optimization, *BMC cancer*, 11 (2011) 143.

773 [37] A.J. Minn, G.P. Gupta, D. Padua, P. Bos, D.X. Nguyen, D. Nuyten, B.
774 Kreike, Y. Zhang, Y. Wang, H. Ishwaran, J.A. Foekens, M. van de Vijver, J.
775 Massagué, Lung metastasis genes couple breast tumor size and metastatic
776 spread, *Proceedings of the National Academy of Sciences of the United*
777 *States of America*, 104 (2007) 6740-6745.

778 [38] L.J. van 't Veer, H. Dai, M.J. van de Vijver, Y.D. He, A.A. Hart, M. Mao,
779 H.L. Peterse, K. van der Kooy, M.J. Marton, A.T. Witteveen, G.J. Schreiber,
780 R.M. Kerkhoven, C. Roberts, P.S. Linsley, R. Bernards, S.H. Friend, Gene
781 expression profiling predicts clinical outcome of breast cancer, *Nature*, 415
782 (2002) 530-536.

783 [39] M. Chanrion, V. Negre, H. Fontaine, N. Salvetat, F. Bibeau, G. Mac
784 Grogan, L. Mauriac, D. Katsaros, F. Molina, C. Theillet, J.M. Darbon, A gene
785 expression signature that can predict the recurrence of tamoxifen-treated
786 primary breast cancer, *Clinical cancer research : an official journal of the*
787 *American Association for Cancer Research*, 14 (2008) 1744-1752.

788 [40] M. Sakaki-Yumoto, C. Kobayashi, A. Sato, S. Fujimura, Y. Matsumoto,
789 M. Takasato, T. Kodama, H. Aburatani, M. Asashima, N. Yoshida, R.
790 Nishinakamura, The murine homolog of SALL4, a causative gene in Okihiro
791 syndrome, is essential for embryonic stem cell proliferation, and cooperates
792 with Sall1 in anorectal, heart, brain and kidney development, *Development*
793 (Cambridge, England), 133 (2006) 3005-3013.

794 [41] J. Yang, L. Chai, F. Liu, L.M. Fink, P. Lin, L.E. Silberstein, H.M. Amin,
795 D.C. Ward, Y. Ma, Bmi-1 is a target gene for SALL4 in hematopoietic and
796 leukemic cells, *Proceedings of the National Academy of Sciences of the*
797 *United States of America*, 104 (2007) 10494-10499.

798 [42] T. Oikawa, A. Kamiya, M. Zeniya, H. Chikada, A.D. Hyuck, Y.
799 Yamazaki, E. Wauthier, H. Tajiri, L.D. Miller, X.W. Wang, L.M. Reid, H.
800 Nakauchi, Sal-like protein 4 (SALL4), a stem cell biomarker in liver cancers,
801 *Hepatology (Baltimore, Md.)*, 57 (2013) 1469-1483.

802 [43] H.L. Goel, T. Gritsko, B. Pursell, C. Chang, L.D. Shultz, D.L. Greiner,
803 J.H. Norum, R. Toftgard, L.M. Shaw, A.M. Mercurio, Regulated splicing of
804 the alpha6 integrin cytoplasmic domain determines the fate of breast cancer
805 stem cells, *Cell reports*, 7 (2014) 747-761.

806 [44] C. Chang, H.L. Goel, H. Gao, B. Pursell, L.D. Shultz, D.L. Greiner, S.
807 Ingerpuu, M. Patarroyo, S. Cao, E. Lim, J. Mao, K.K. McKee, P.D. Yurchenco,
808 A.M. Mercurio, A laminin 511 matrix is regulated by TAZ and functions as
809 the ligand for the alpha6Bbeta1 integrin to sustain breast cancer stem cells,
810 *Genes & development*, 29 (2015) 1-6.

811 [45] H. Lahlou, W.J. Muller, beta1-integrins signaling and mammary tumor
812 progression in transgenic mouse models: implications for human breast
813 cancer, *Breast cancer research : BCR*, 13 (2011) 229.

814 [46] A. Kondo, S. Hashimoto, H. Yano, K. Nagayama, Y. Mazaki, H. Sabe, A
815 new paxillin-binding protein, PAG3/Papalpha/KIAA0400, bearing an

816 ADP-ribosylation factor GTPase-activating protein activity, is involved in
817 paxillin recruitment to focal adhesions and cell migration, *Molecular biology*
818 *of the cell*, 11 (2000) 1315-1327.

819 [47] S.M. Pontier, W.J. Muller, Integrins in mammary-stem-cell biology and
820 breast-cancer progression--a role in cancer stem cells?, *Journal of cell science*,
821 122 (2009) 207-214.

822 [48] H. Tatetsu, N.R. Kong, G. Chong, G. Amabile, D.G. Tenen, L. Chai,
823 SALL4, the missing link between stem cells, development and cancer, *Gene*,
824 584 (2016) 111-119.

825 [49] K.J. Yong, C. Gao, J.S. Lim, B. Yan, H. Yang, T. Dimitrov, A. Kawasaki,
826 C.W. Ong, K.F. Wong, S. Lee, S. Ravikumar, S. Srivastava, X. Tian, R.T.
827 Poon, S.T. Fan, J.M. Luk, Y.Y. Dan, M. Salto-Tellez, L. Chai, D.G. Tenen,
828 Oncofetal gene SALL4 in aggressive hepatocellular carcinoma, *The New*
829 *England journal of medicine*, 368 (2013) 2266-2276.

830

831 **Figure legends**

832 **Fig. 1.** SALL4 is required for the spindle-shaped morphology and cell migration. (A)
833 Controls and SALL4 knockdowns of SUM159 and MDA-MB-231 cells are shown. (B)
834 Images of migrated cells are shown. Cell nuclei were stained with Hoechst 33342.
835 Arrowheads indicate the signals of migrated cells. For simplicity, not all signals are
836 pointed. (C) Graphs show the number of migrated cells ($n = 4$). The vertical axis
837 indicates the number of migrated cells. (D) Cells were stained with an
838 anti-phosphorylated paxillin antibody. Arrowheads indicate the immunoreactions. For
839 simplicity, not all signals are pointed. (E) Graphs show the ratio of the FA-rich region.
840 The vertical axis indicates the value obtained by dividing the length of the FA-rich
841 region by the perimeter. The cell numbers were 31 in SUM159;shGFP, 36 in
842 SUM159;shSALL4, 40 in MDA-MB-231;shGFP and 41 in MDA-MB-231;shSALL4
843 cells. (F) Images of immunostaining with anti-GM130 are shown. (G) Ratios of
844 polarized cells are shown in the graph. The vertical axis indicates the percentage of
845 polarized cells. The cell numbers were 195 in SUM159;shGFP, 249 in
846 SUM159;shSALL4, 163 in MDA-MB-231;shGFP and 162 in MDA-MB-231;shSALL4

847 cells. Scale bars indicate 100 μm in A,B, and 20 μm in D,F. Student's *t*-test was used in
848 C,E. Fisher's exact test was used in G. n.s.: not significant, **: $P < 0.01$. Error bars
849 represent the standard deviation.

850

851 **Fig. 2.** SALL4 up-regulates integrin $\alpha 6$ and $\beta 1$ expression. (A) The scatter plot shows
852 the gene expressions in the control and SALL4 knockdown SUM159 cells. Integrin
853 genes reduced by SALL4 knockdown are indicated. The accession numbers of the
854 shGFP and shSALL4 data are DRA004721 and DRA004722, respectively. (B) Relative
855 expression levels of integrin family genes are shown ($n = 3$). In each gene, mean
856 expression level of the shGFP cells was defined as 1. Arrowheads point the genes that
857 had expression reduced to less than half of that of the controls by SALL4 knockdown in
858 both SUM159 and MDA-MB-231 cells. (C) Images show cells with integrin $\alpha 6$ and $\beta 1$
859 knockdown. (D) The results of the Boyden chamber assays are shown ($n = 4$).
860 MDA-MB-231 cells were used. The vertical axis indicates the number of migrated cells.
861 (E) Reporter assays using the integrin $\alpha 6$ and $\beta 1$ gene promoters were performed ($n =$
862 4). The vertical axis indicates the relative light units of luciferase. The mean value of

863 the FLAG control was defined as 1. (F) Enrichment of the integrin $\alpha 6$ and $\beta 1$ promoter
864 region is shown. MDA-MB-231 cells were used. Chromatin immunoprecipitation
865 samples were used for PCR amplification with primers for the integrin $\alpha 6$ and $\beta 1$
866 promoters. ChIP: chromatin immunoprecipitation. Scale bars indicate 100 μm .
867 Student's *t*-test was used for statistical analyses. *: $P < 0.05$, **: $P < 0.01$. Error bars
868 represent the standard deviation.

869

870 **Fig. 3.** SALL4-regulated integrin $\alpha 6$ and $\beta 1$ expression is required for spindle-shaped
871 morphology and cell migration in basal-like breast cancer cells. (A) Boyden chamber
872 assays were performed with cells overexpressing integrin $\alpha 6$ and $\beta 1$ ($n = 4$ in control, n
873 $= 5$ in the $\alpha 6$ and $\beta 1$ overexpressing groups). The vertical axis indicates the number of
874 migrated cells. (B) Cells overexpressing integrin $\alpha 6$ and $\beta 1$ are shown. (C) Images of
875 immunostaining with anti-phosphorylated paxillin are shown. Arrowheads indicate the
876 immunoreaction signals. For simplicity, not all signals are pointed. (D) Graphs show the
877 ratio of the FA-rich region. The cell numbers were 33 in control;shGFP, 36 in
878 control;shSALL4, 45 in $\alpha 6\text{v}1,\beta 1$;shGFP, 37 in $\alpha 6\text{v}1,\beta 1$;shSALL4, 39 in

879 $\alpha6v2,\beta1;shGFP$ and 33 in $\alpha6v2,\beta1;shSALL4$. (E) Immunoblotting for FAK was
880 performed. (F) The intensity of phosphorylated FAK and the total FAK bands were
881 measured. Relative FAK phosphorylation levels to shGFP are graphed ($n = 3$). Scale
882 bars indicate 100 μm in B, and 20 μm in C. Student's t -test was used. *: $P < 0.05$, **: P
883 < 0.01 . Error bars represent the standard deviation.

884

885 **Fig. 4.** Integrin $\alpha6$ and $\beta1$ form a heterodimer. (A) Co-immunoprecipitation samples
886 were used for immunoblotting with an anti-integrin $\beta1$ antibody. IP:
887 immunoprecipitation. IB: immunoblotting. (B) Confocal images of immunostained cells
888 are shown. Antibodies for integrin $\alpha6$ and $\beta1$ were used for double-immunostaining.
889 (C-F) Binding assays were performed ($n = 4$). The number of cells bound to the BSA
890 blocking solution and the recombinant laminin-511 E8 fragment are shown in C,E and
891 D,F, respectively. The vertical axis indicates the number of bound cells. SUM159 and
892 MDA-MB-231 cells were used in C,D. MDA-MB-231 cells overexpressing integrin $\alpha6$
893 and $\beta1$ were used in E,F. Scale bars indicate 20 μm . Student's t -test was used. n.s.: not
894 significant, **: $P < 0.01$. Error bars represent the standard deviation.

895

896 **Fig. 5.** SALL4 activates the FA dynamics. (A) Cells with a paxillin-EGFP fusion were
897 used to monitor the FA dynamics. Images of shScr (control) and shSALL4 cells are
898 shown. Yellow and blue arrowheads indicate the FA signals assembled and
899 disassembled in 10 min, respectively. For simplicity, not all signals are pointed. (B) The
900 ratio of assembled FAs was calculated by dividing the number of newly formed FA in
901 10 min by the total FA number at 10 min. (C) The ratio of disassembled FA was
902 calculated by dividing the number of FAs lost in 10 min by the total FA number at 0
903 min. The cell numbers analyzed in B,C were 33 in the control;shGFP, 36 in the
904 control;shSALL4, 31 in $\alpha6v1,\beta1$;shGFP, 37 in $\alpha6v1,\beta1$;shSALL4, 41 in
905 $\alpha6v2,\beta1$;shGFP and 47 in $\alpha6v2,\beta1$;shSALL4 cells. Scale bars indicate 20 μ m.
906 Student's *t*-test was used. **: $P < 0.01$. Error bars represent the standard deviation.

907

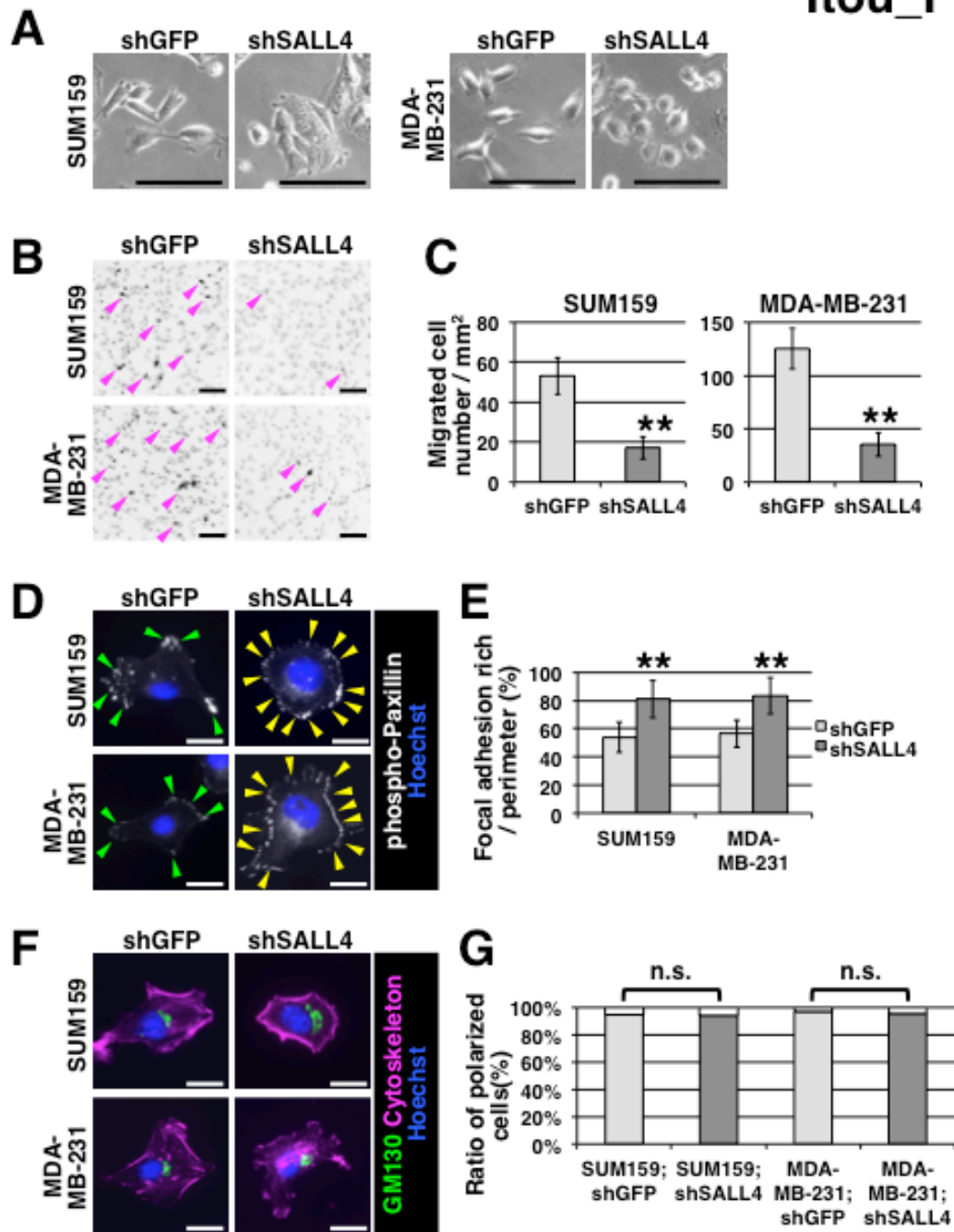
908 **Fig. 6.** The SALL4 - integrin $\alpha6\beta1$ network modulates Rho activity to promote cell
909 migration. (A) RhoA protein level was not changed by SALL4 knockdown in
910 MDA-MB-231 cells. (B) RhoA activity was measured with RhoA G-LISA Activation

911 **Assay Kit.** Relative RhoA activity to shGFP was calculated ($n = 3$). (C)
912 Immunofluorescence images of phosphorylated paxillin are shown. A ROCK inhibitor,
913 Y-27632, was used. Arrowheads indicate the signals. For simplicity, not all signals are
914 pointed. (D) The FA-rich region was analyzed. The cell numbers analyzed were 43 in
915 SUM159;shGFP, 35 in SUM159;shSALL4 with water, 43 in SUM159;shSALL4 with
916 the ROCK inhibitor, 41 in MDA-MB-231;shGFP, 36 in MDA-MB-231;shSALL4 with
917 water and 31 in MDA-MB-231;shSALL4 with the ROCK inhibitor. (E) Boyden
918 chamber assays were performed with the ROCK inhibitor ($n = 4$). The vertical axis
919 indicates the number of migrated cells. Scale bars indicate 20 μm . Student's *t*-test was
920 used. **: $P < 0.01$. Error bars represent the standard deviation.

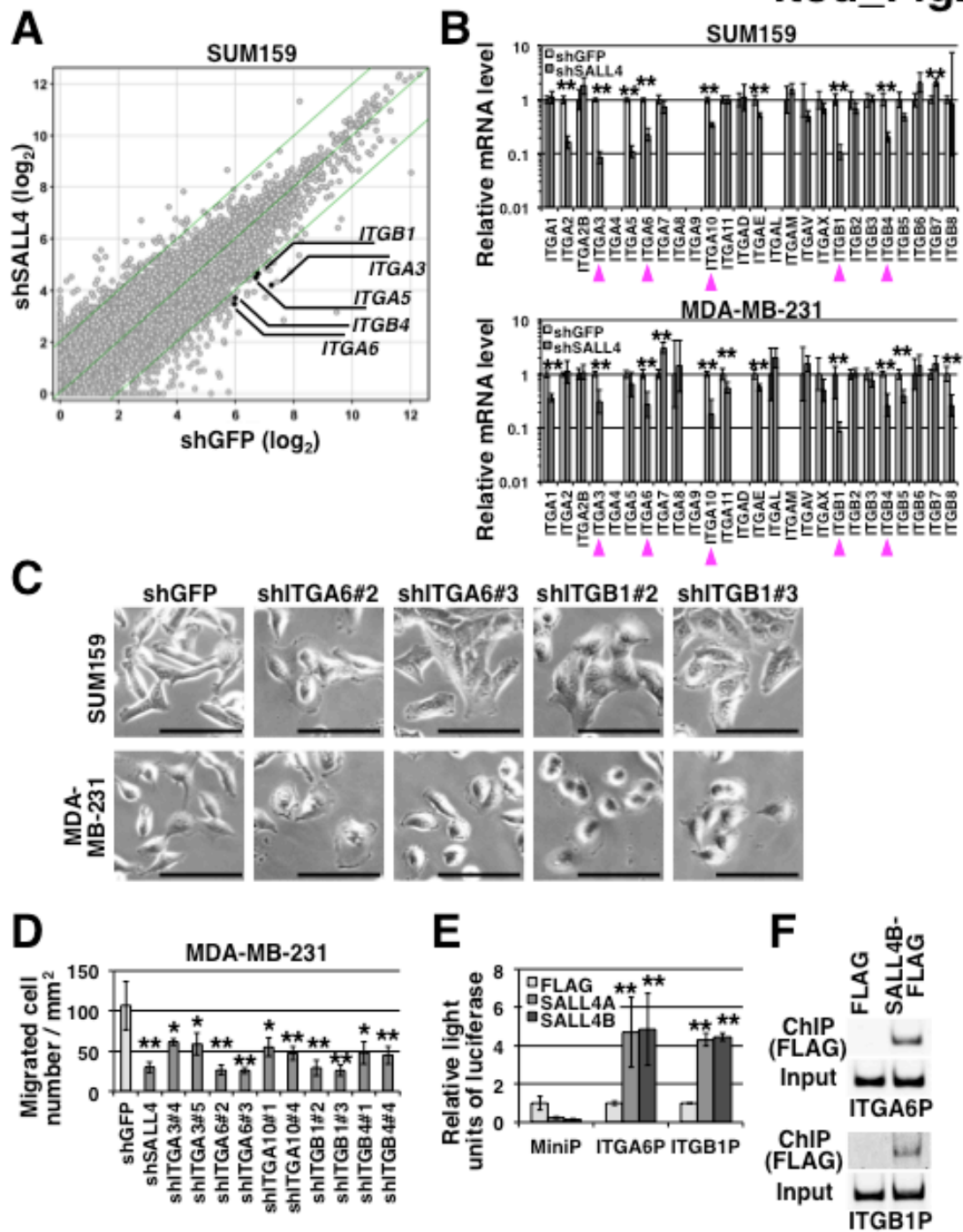
921

922 **Fig. 7.** The SALL4 - integrin $\alpha 6\beta 1$ network is required for *in vivo* cell migration. (A)
923 Metastasis tracking assay of transplanted SUM159 cells in zebrafish larvae. In the
924 control condition (shGFP), the SUM159 cells (magenta) moved to the anterior (yellow
925 square) and posterior (blue square) from the injected site at day 3. The metastasized
926 cells (arrowheads) were localized outside of the vasculatures (green, *fli1-EGFP*). On the

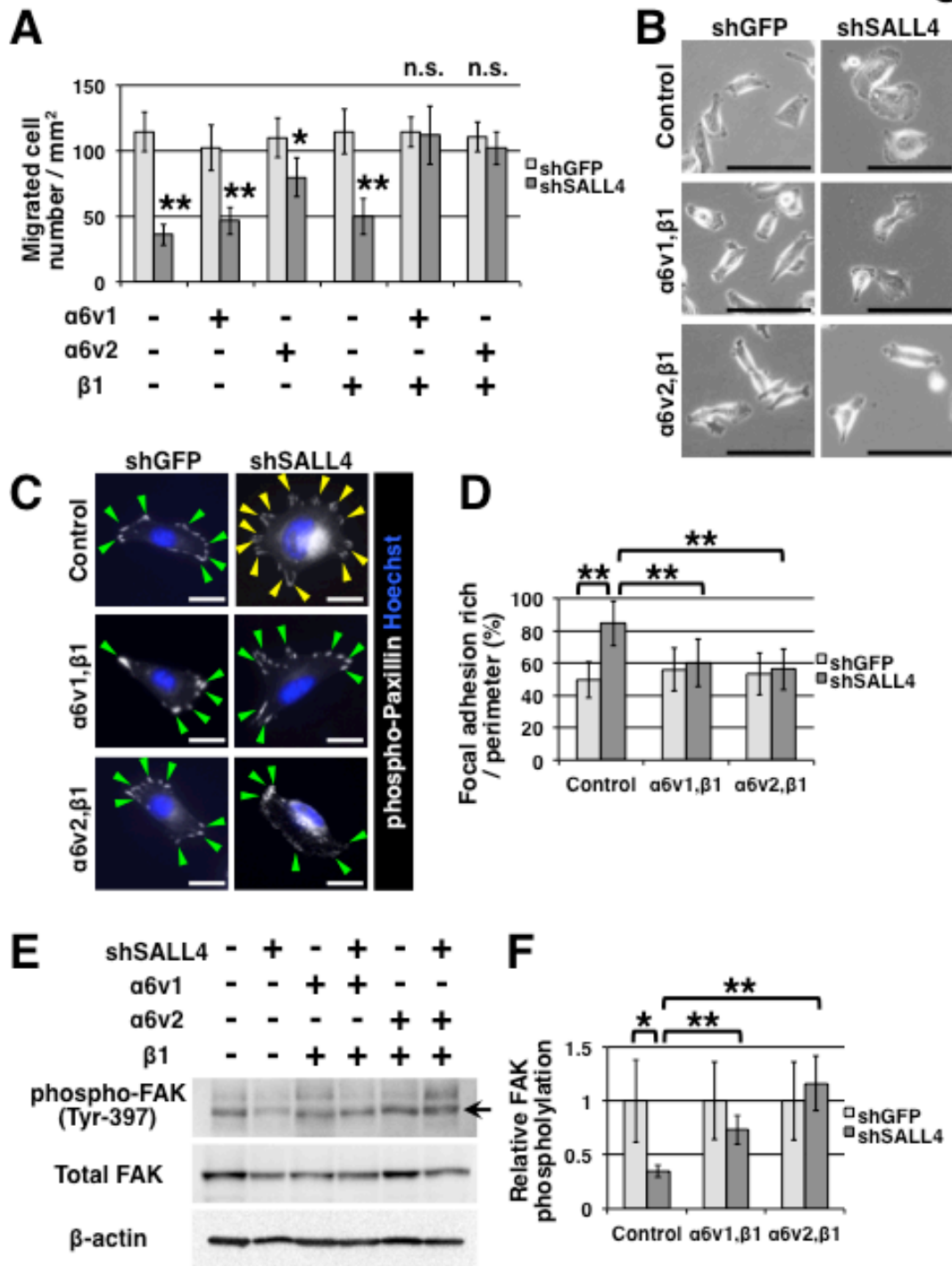
927 other hand, the SALL4 knockdown cells did not migrate out from the abdominal cavity.
928 Scale bars indicate 500 μm . (B,C) Statistical data for the metastasis assay. The ratio of
929 fish with the metastasis was decreased under the shSALL4 condition in the both of
930 SUM159 and MDA-MB-231 cells (B). The shSALL4-induced phenotype was rescued
931 by overexpression of integrin $\alpha 6$ and $\beta 1$ (C). Fisher's exact test was used. **: $P < 0.01$.



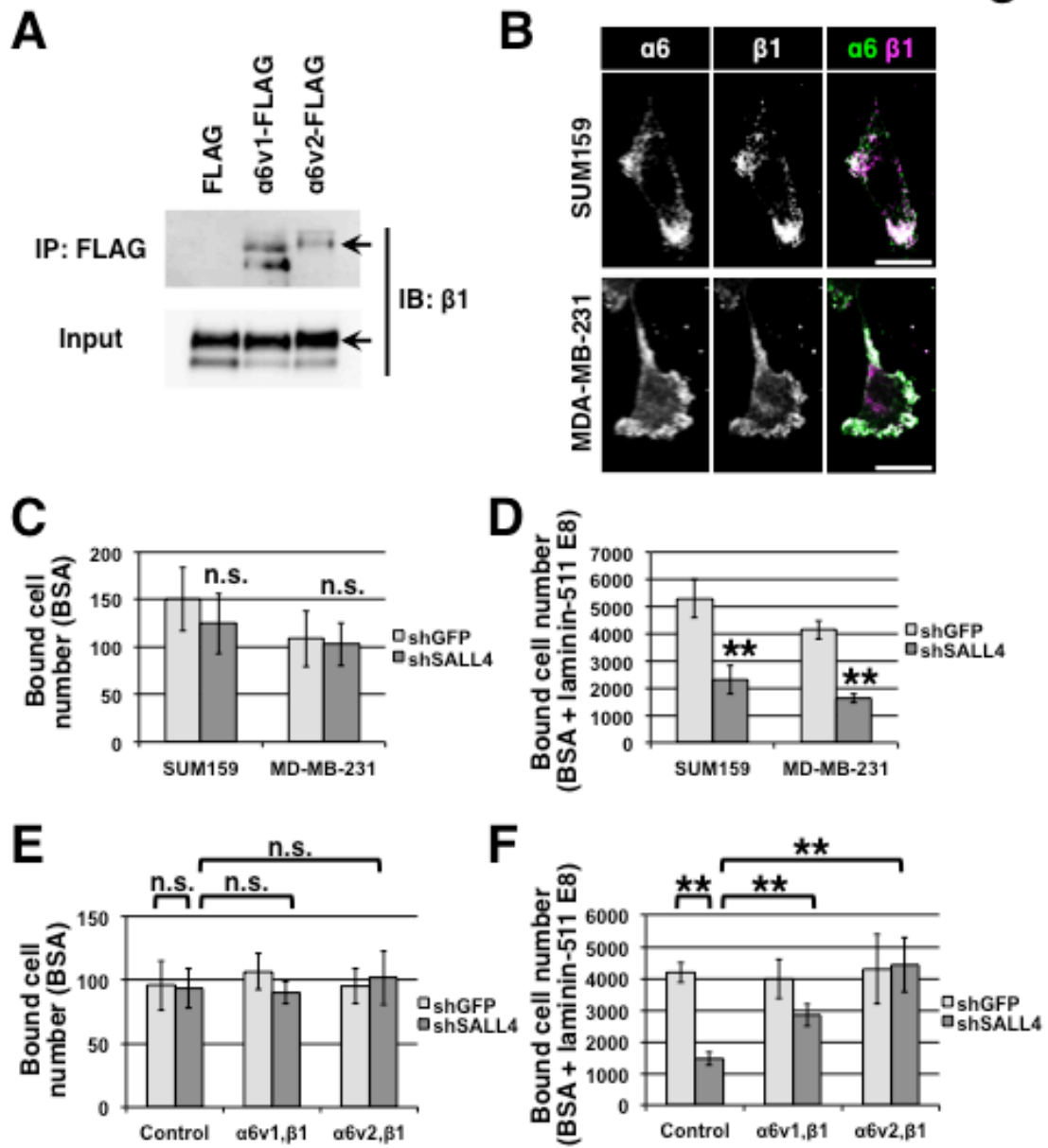
Itou_Fig2

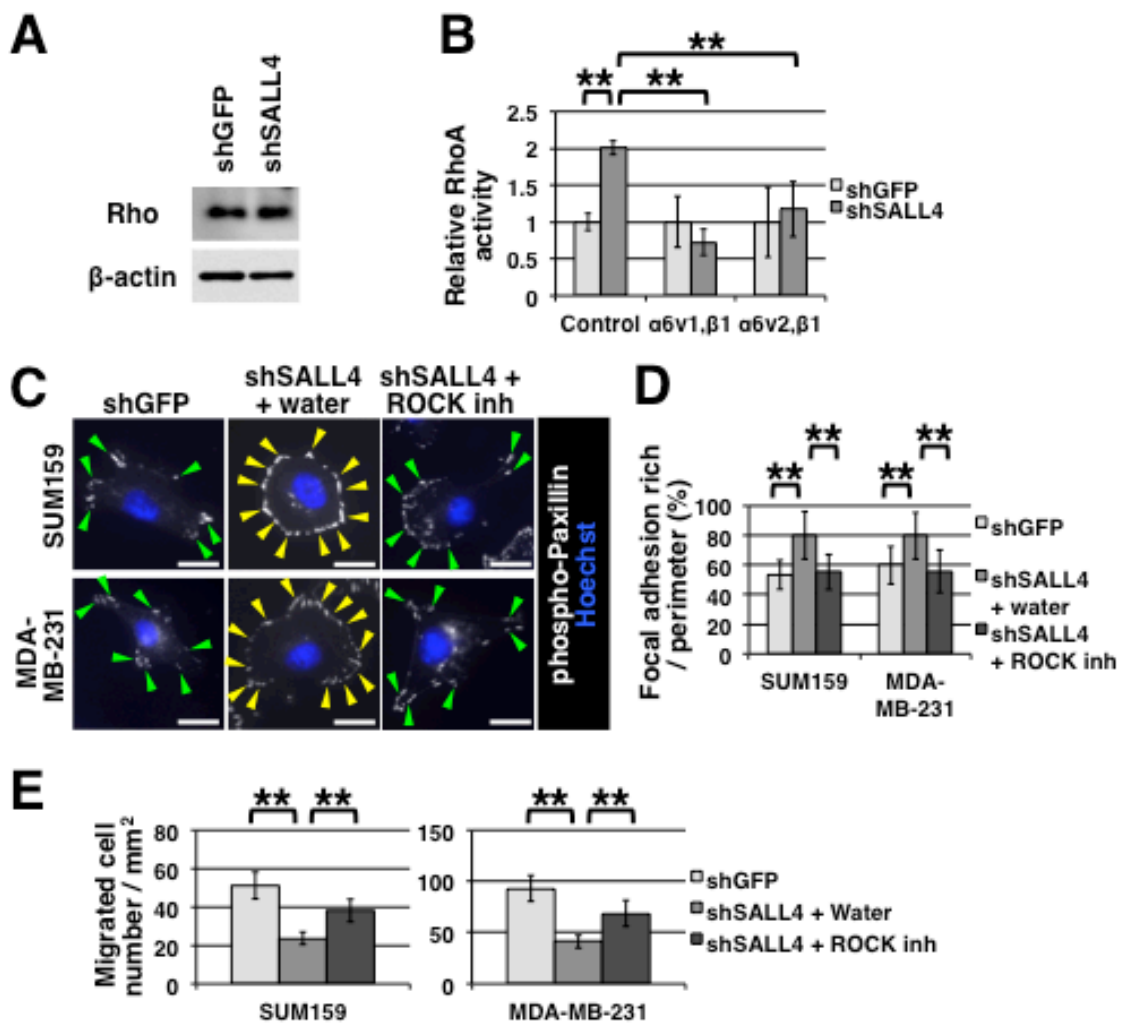
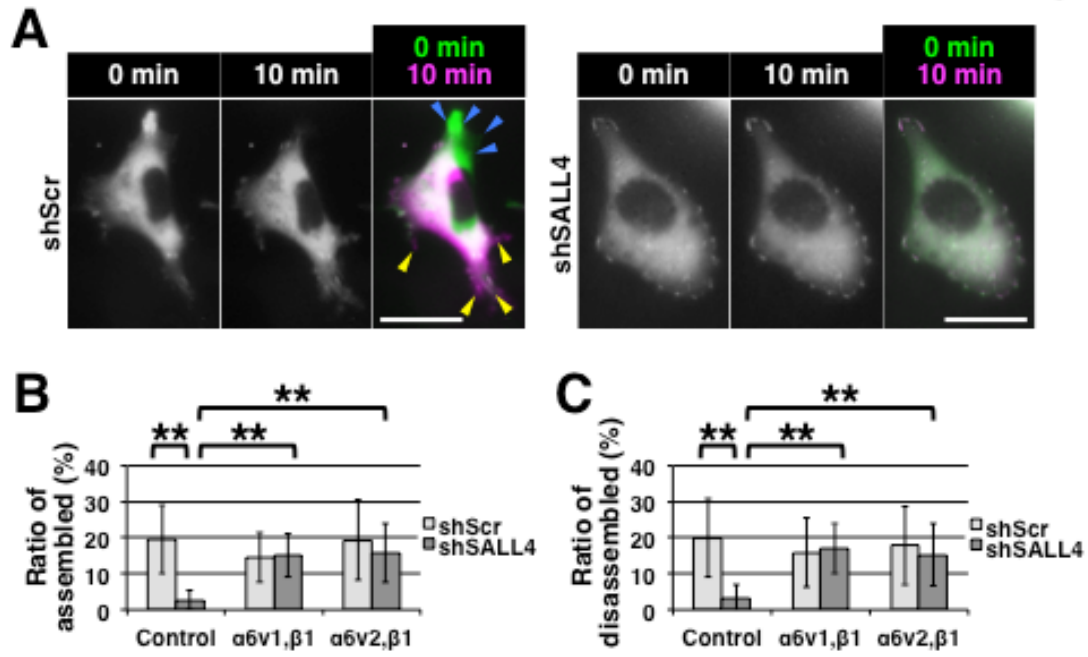


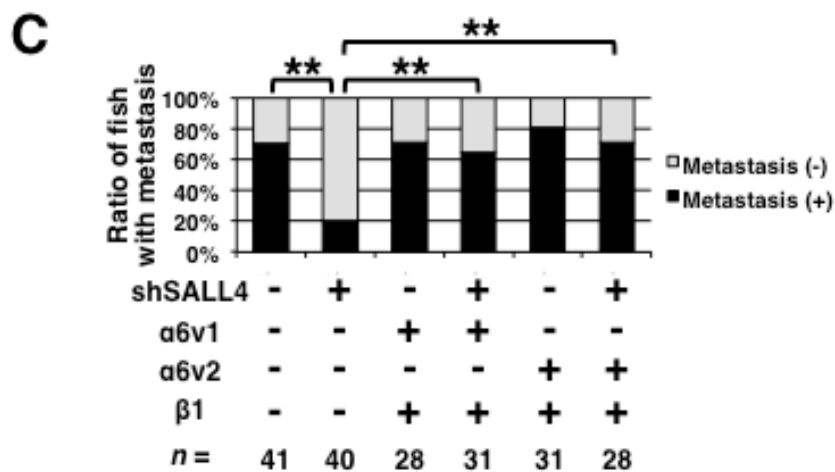
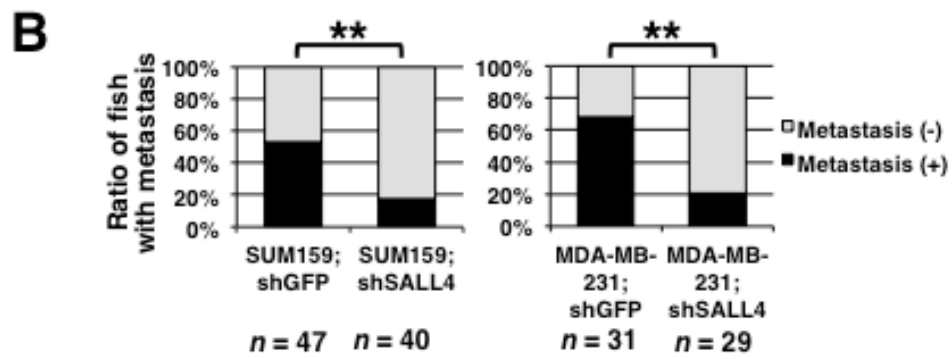
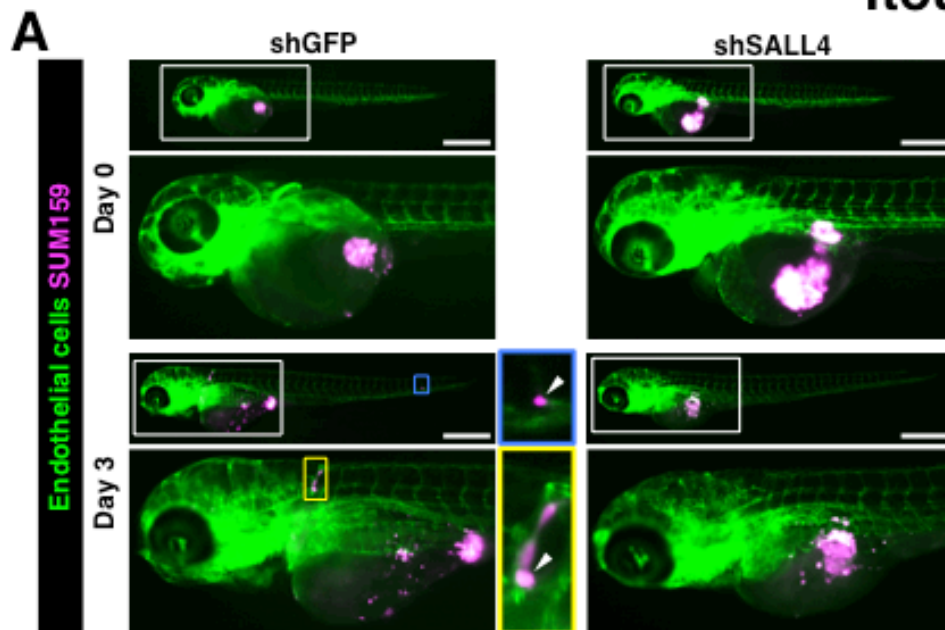
Itou_Fig3



Itou_Fig4







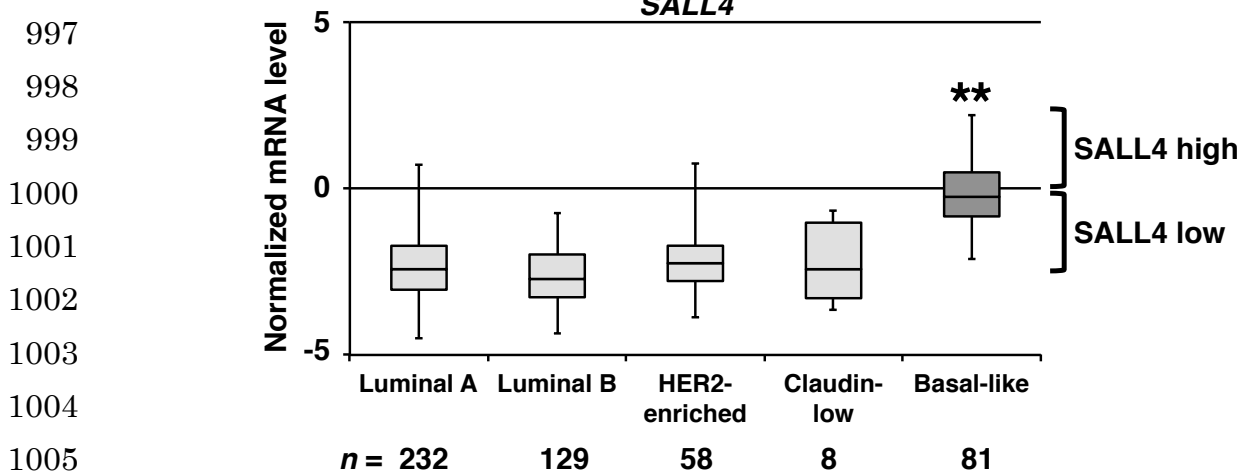
938 **The Sal-like 4 - integrin $\alpha6\beta1$ network promotes cell migration for metastasis via**
939 **activation of focal adhesion dynamics in basal-like breast cancer cells.**
940
941 Junji Itou, Sunao Tanaka, Wenzhao Li, Atsuo Iida, Atsuko Sehara-Fujisawa, Fumiaki
942 Sato, Masakazu Toi
943
944
945 **Supplementary Fig. S1.** The FA-rich region and the perimeter were measured.
946 **Supplementary Fig. S2.** Knockdown of integrin $\alpha3$, $\alpha10$ and $\beta4$ causes no remarkable
947 morphological change.
948 **Supplementary Fig. S3.** Breast cancer patients with high SALL4 expression have high
949 integrin $\alpha6$ and $\beta1$ expression.
950 **Supplementary Fig. S4.** Integrin $\alpha6$ and $\beta1$ overexpression constructs were introduced
951 into MDA-MB-231 cells.
952 **Supplementary Fig. S5.** Rho inhibition reverses cell morphology of the SALL4
953 knockdown cells.
954 **Supplementary Fig. S6.** The SALL4 - integrin $\alpha6\beta1$ network augments migration
955 through modulation of Rho activity.
956 **Supplementary Fig. S7.** SALL4 knockdown impairs cell growth and tumor formation.
957 **Supplementary Fig. S8.** Co-expression of integrin $\alpha6$ and $\beta1$ genes causes poor
958 metastasis-free survival in some cases.
959 **Supplementary Table S1.** List of shRNA sequences
960 **Supplementary Table S2.** Primer sequences for qRT-PCR
961

994

995

996

A



1000

1001

1002

1003

1004

1005

1006

1007

B

1008

1009

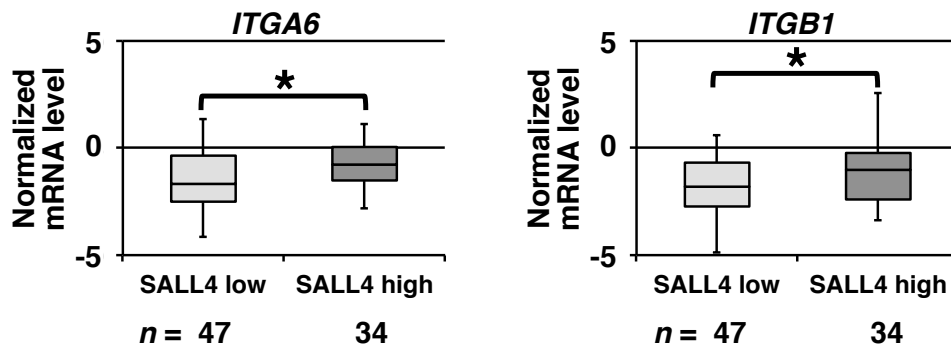
1010

1011

1012

1013

1014



1015

1016

1017

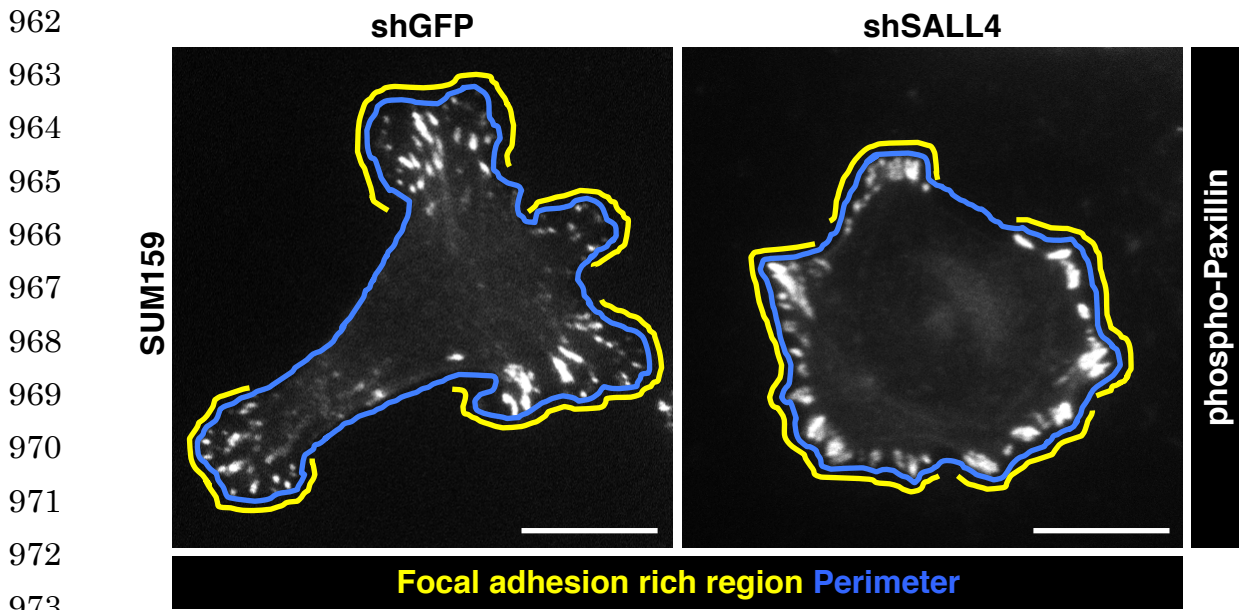
1018

1019

1020

1021

Supplementary Fig. S3. Breast cancer patients with high SALL4 expression have high integrin $\alpha 6$ and $\beta 1$ expression. (A) SALL4 expression levels in breast cancer subtypes are graphed. (B) The expression level of the integrin $\alpha 6$ and $\beta 1$ genes is shown. A Kruskal-Wallis H test was used in A. A Mann-Whitney U test was used in B. *: $P < 0.05$, **: $P < 0.01$. In the box plots, values of 25%, the median and 75% are indicated. Error bars represent the range between the minimum and maximum values.



974 **Supplementary Fig. S1.** The FA-rich region and the perimeter were measured.
 975 Phosphorylated paxillin immunostaining is shown. Yellow and blue lines indicate the
 976 FA-rich region and the perimeter, respectively. Scale bars indicate 20 μm .

977

978

979

980

981

982

983

984

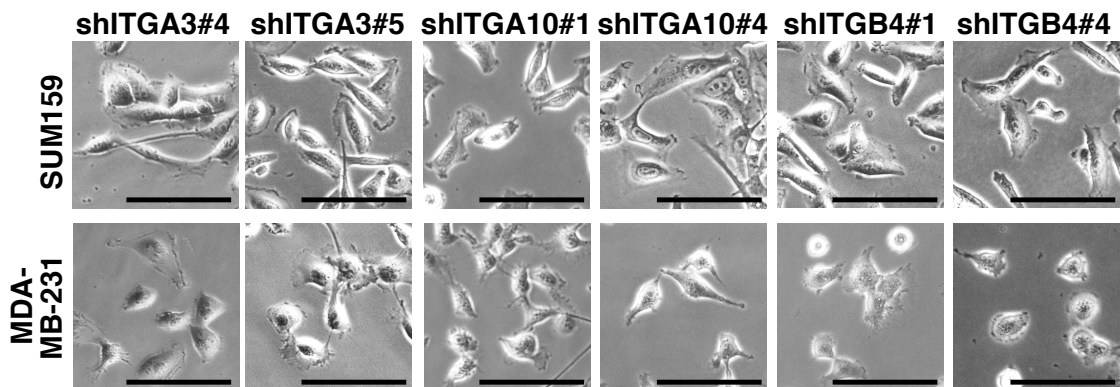
985

986

987

988

989



990 **Supplementary Fig. S2.** Knockdown of integrin $\alpha 3$, $\alpha 10$ and $\beta 4$ causes no remarkable
 991 morphological change. Images of the knockdown cells are shown. SUM159 and
 992 MDA-MB-231 cells were used. Scale bars indicate 100 μm .

993

1022

1023

1024

1025

1026

1027

1028

1029

1030

1031

1032

1033

1034

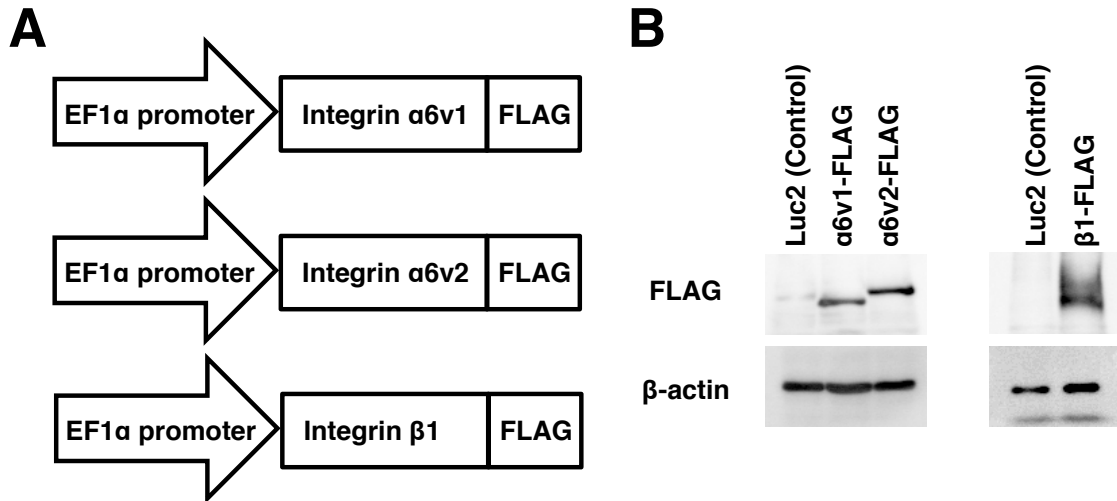
1035 **Supplementary Fig. S4.** Integrin $\alpha 6$ and $\beta 1$ overexpression constructs were introduced

1036 into MDA-MB-231 cells. (A) Constructs for overexpressing $\alpha 6v1$, $\alpha 6v2$ and $\beta 1$ are

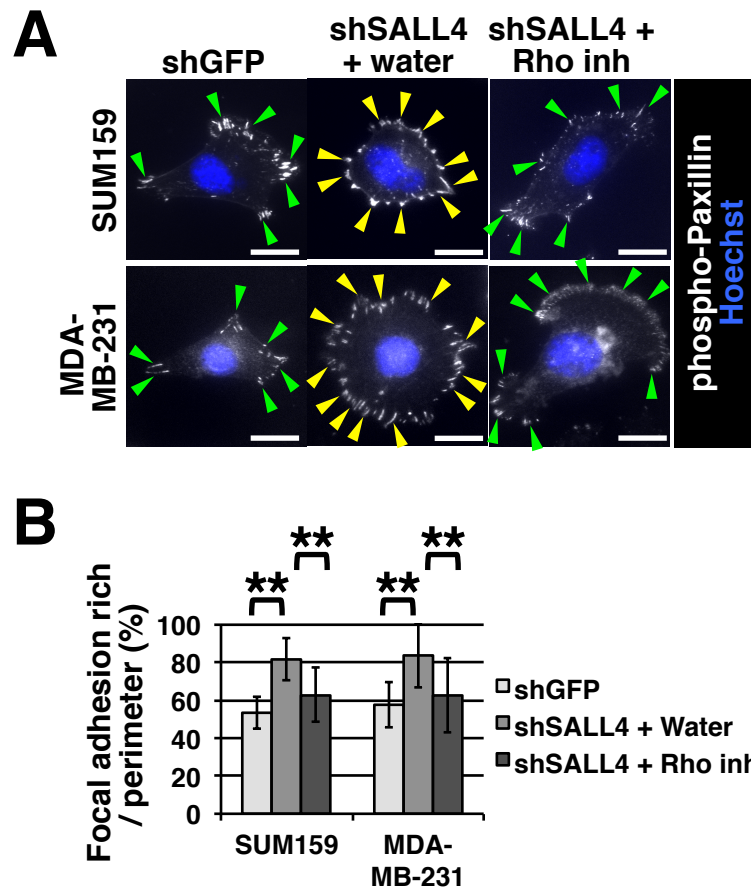
1037 depicted. (B) Immunoblotting was performed to confirm expression from the constructs.

1038 An anti-FLAG antibody was used.

1039

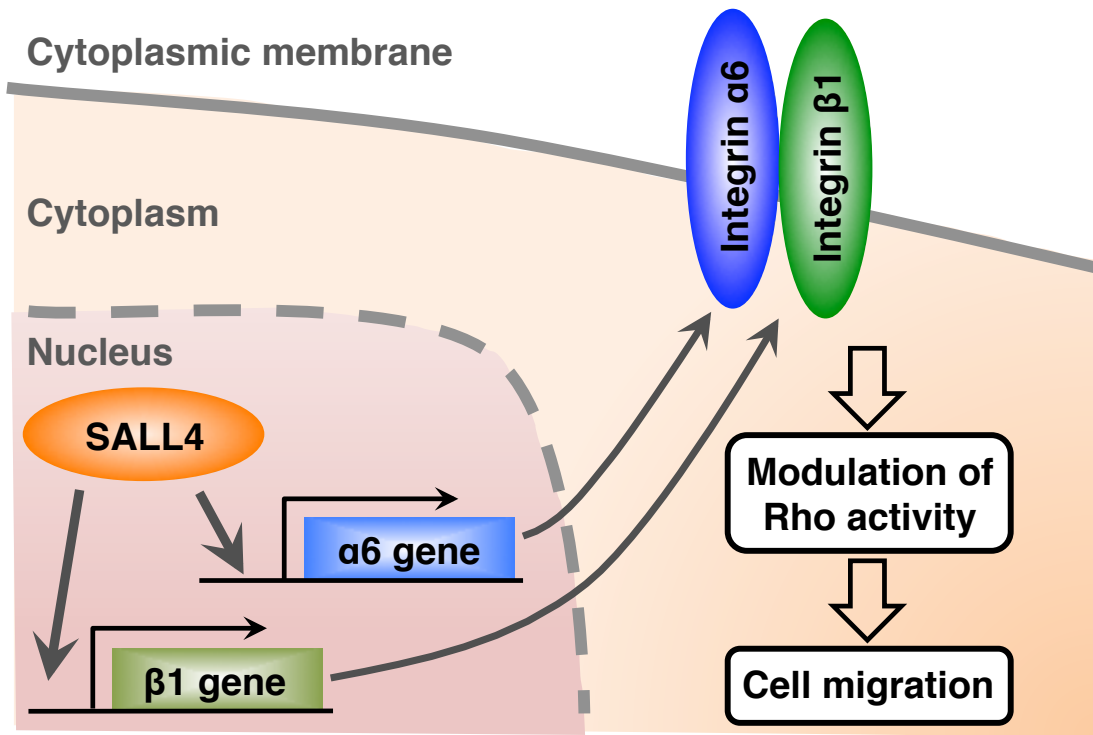


1040
 1041
 1042
 1043
 1044
 1045
 1046
 1047
 1048
 1049
 1050
 1051
 1052
 1053
 1054
 1055
 1056
 1057
 1058
 1059
 1060
 1061
 1062
 1063
 1064
 1065
 1066
 1067
 1068



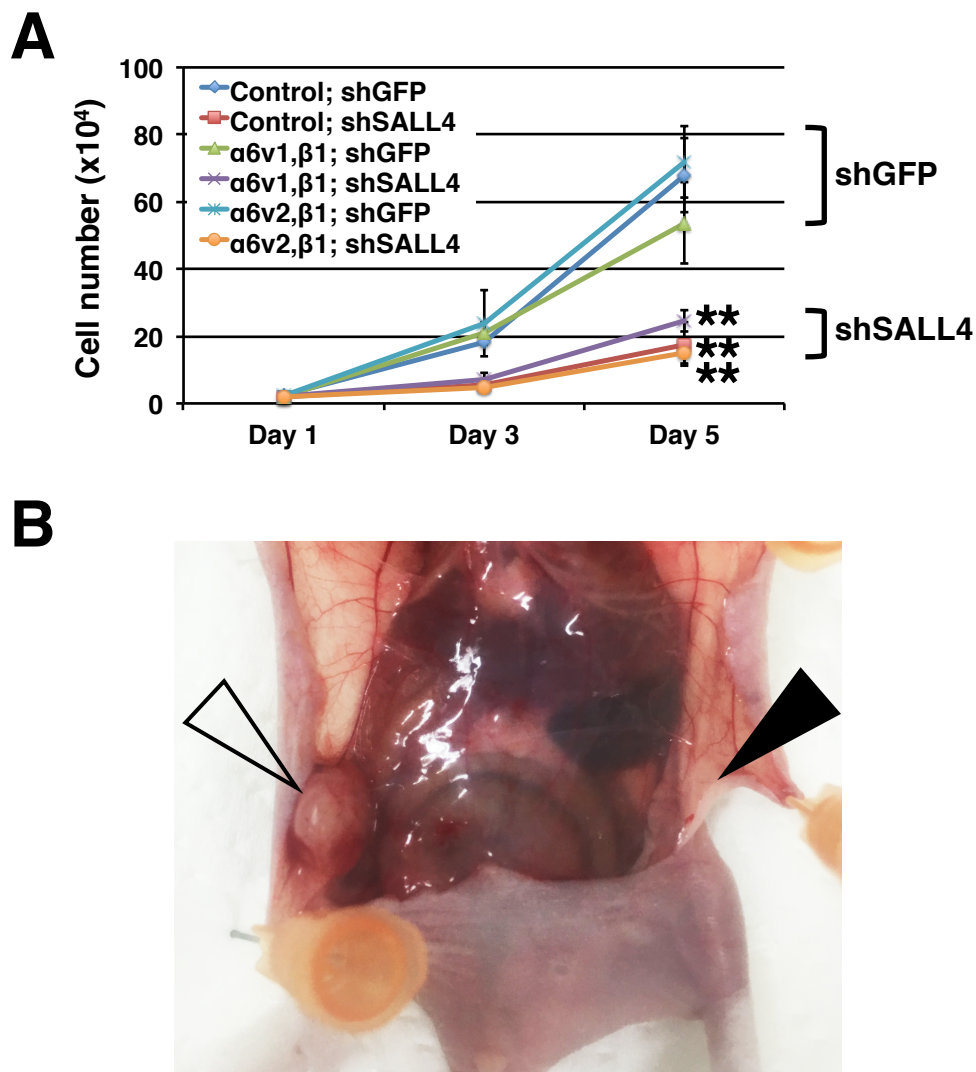
Supplementary Fig. S5. Rho inhibition reverses cell morphology of the SALL4 knockdown cells. (A) Images show immunostaining with an anti-phosphorylated paxillin antibody. A Rho inhibitor, C3 transferase, was used. Arrowheads indicate the signals. For simplicity, not all signals are pointed. (B) The FA-rich region was analyzed. The cell numbers analyzed were 38 in SUM159;shGFP, 35 in SUM159;shSALL4 with water, 37 in SUM159;shSALL4 with the Rho inhibitor, 34 in MDA-MB-231;shGFP, 38 in MDA-MB-231;shSALL4 with water and 38 in MDA-MB-231;shSALL4 with the Rho inhibitor. Scale bars indicate 20 μ m. Student's *t*-test was used. **: $P < 0.01$. Error bars represent the standard deviation.

1069
1070
1071
1072
1073
1074
1075
1076
1077
1078
1079
1080
1081
1082
1083
1084
1085
1086
1087
1088
1089
1090



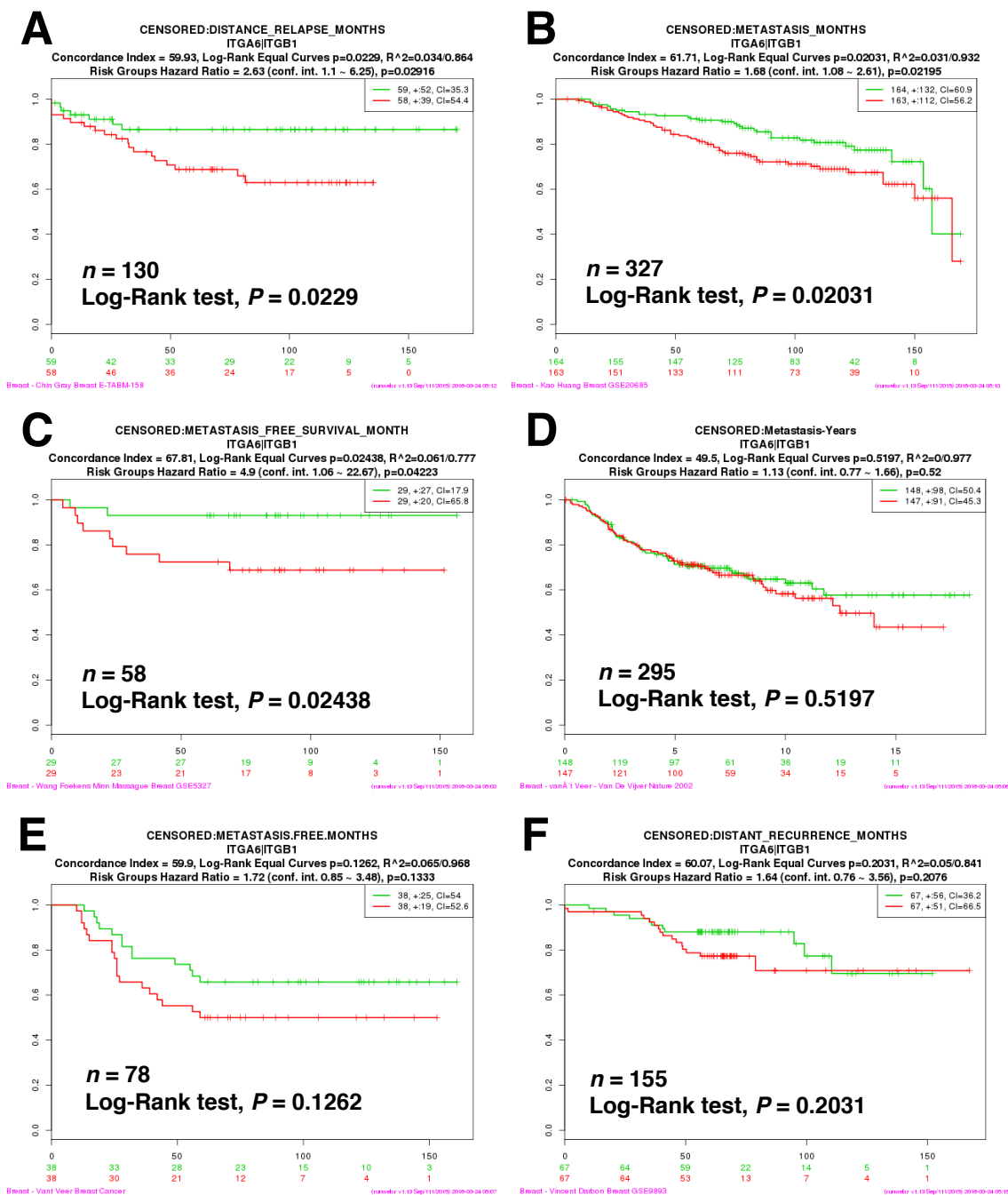
Supplementary Fig. S6. The SALL4 - integrin $\alpha6\beta1$ network augments migration through modulation of Rho activity. In the nucleus, SALL4 binds to the promoters of the integrin $\alpha6$ and $\beta1$ genes, and up-regulates their expression. Integrin $\alpha6$ and $\beta1$ form a heterodimer, and modulate Rho activity. This network promotes cell migration in basal-like breast cancer cells.

1091
1092
1093
1094
1095
1096
1097
1098
1099
1100
1101
1102
1103
1104
1105
1106
1107
1108
1109
1110
1111
1112
1113
1114
1115
1116
1117
1118
1119
1120
1121



Supplementary Fig. S7. SALL4 knockdown impairs cell growth and tumor formation. (A) The cell number was counted on days 1, 3 and 5. Statistical analyses were performed on day 5 between the shGFP and shSALL4 groups in control, $\alpha 6v1, \beta 1$, and $\alpha 6v2, \beta 1$ cells. Student's *t*-test was used. **: $P < 0.01$. Error bars represent the standard deviation. (B) Typical image of mouse xenograft experiments with control and SALL4 knockdown cells. The transplanted site of SALL4 knockdown cells showed no visible tumor formation at 1 month-post-transplantation (filled arrowhead), whereas a tumor was observed in the site where control cells were injected (open arrowhead).

1122
 1123
 1124
 1125
 1126
 1127
 1128
 1129
 1130
 1131
 1132
 1133
 1134
 1135
 1136
 1137
 1138
 1139
 1140
 1141
 1142
 1143
 1144
 1145
 1146
 1147
 1148
 1149
 1150
 1151
 1152
 1153
 1154



Supplementary Fig. S8. Co-expression of integrin $\alpha 6$ and $\beta 1$ genes causes poor metastasis-free survival in some cases. (A-F) The correlation between integrin $\alpha 6$ and $\beta 1$ expression and metastasis-free survival was analyzed using the SurvExpress platform. Red and green lines indicate groups with high and low integrin $\alpha 6$ and $\beta 1$ expression, respectively. The log-rank test was used. The database names are Chin Gray Breast E-TAB-158 (A), Kao Huang Breast GSE20685 (B), Wang Foekens Minn Massague Breast GSE5327 (C), van't Veer - Van De Vijver Nature 2002 (D), Vant Veer Breast Cancer (E), and Vincent Darbon Breast GSE9893 (F).

1155 **Supplementary Table S1. List of shRNA sequences**

Name	Target sequence (5' → 3')
shGFP	GCACGACTTCTTCAAGTCCGC
shScr	CCTAAGGTTAAGTCGCCCTCG
shSALL4	GTGAGGATGAAGCCACAGTAA
shITGA3#4	CCAGGATGGATTTTCAGGATAT
shITGA3#5	CATCGAGGATTACAGAGACTT
shITGA6#2	CGAGAAGGAAATCAAGACAAA
shITGA6#3	CGGATCGAGTTTGATAACGAT
shITGA10#1	CCTGAGAGAAATTAGAACTAT
shITGA10#4	CGGCTAAAGGATGGGATTCTT
shITGB1#2	CCTTGCATTACTGCTGATAT
shITGB1#3	GCACGATGTGATGATTTAGAA
shITGB4#1	CTCCTCAGCTACTCCATCCTT
shITGB4#4	GAGGGTGTCATCACCATTGAA

1156

1157

1158 **Supplementary Table S2. Primer sequences for qRT-PCR**

Name	Direction	Sequence (5' → 3')
ITGA1_F	Forward	CAGGTCATTATCTACAGGATGGAAG
ITGA1_R	Reverse	AGAATCCTTGTC AATGTCAGTTG
ITGA2_F	Forward	CAGAATTTGGAACGGGACTTTTCG
ITGA2_R	Reverse	CTCAGGGTTATAGGTGTTGATTTTC
ITGA2B_F	Forward	CGGTGCTGGCCTTCCTGTGG
ITGA2B_R	Reverse	GGAGGACACGTTGAACCATGCG
ITGA3_F	Forward	CTGATCATCCTCCTGCTGTGG
ITGA3_R	Reverse	GCCTTCTGCCTCTTAGCTTCATAC
ITGA4_F	Forward	CAATAGTATGGCTCCCAATGTTAG
ITGA4_R	Reverse	AGTGGCATTCTCCAGTAGTAG
ITGA5_F	Forward	TGCACCAACAAGAGAGCCAAAG
ITGA5_R	Reverse	CTCACACTGCAGGCTAAATGG
ITGA6_F	Forward	GGACAGCAAGGCGTCTCTTATT
ITGA6_R	Reverse	CGGCAGCAGCAGTCACATCAA
ITGA7_F	Forward	CTCTGGAACAGCACCTTTCTGG
ITGA7_R	Reverse	CTCGGAGCATCAAGTTCTTTATGG
ITGA8_F	Forward	ACTCCCAGAAGGAAGCATAGTA
ITGA8_R	Reverse	TGGCGAGAACCAACAATCCAAG
ITGA9_F	Forward	CTCATGGGAACCCAGAAGAGG
ITGA9_R	Reverse	GAGGATTCCCACCAACAACTG
ITGA10_F	Forward	GAGCTGGGAACCGAAGAGGG
ITGA10_R	Reverse	CCACAGGGAGATGAGGATAG
ITGA11_F	Forward	GCCCCTTCATCTTCCGTGAGGAG
ITGA11_R	Reverse	GGTGCTGCCTACAATGATCC
ITGAD_F	Forward	CCCTGTGTTTCAGAGAGAAAACC
ITGAD_R	Reverse	GCAGTCAGCAATGGAGCAGTC
ITGAE_F	Forward	GCAGAGAACCACAGAACTAAG
ITGAE_R	Reverse	CTTGAACAGGATGACCAGAATCACG
ITGAL_F	Forward	CTCCACACTCTATGTCAGTTTC
ITGAL_R	Reverse	GTGGGTATGTTGTGGTCGTGGATG

ITGAM_F	Forward	TTCAATGCTACCCTCAAAGGC
ITGAM_R	Reverse	GAACACGGAATCGTTAAACAAG
ITGAV_F	Forward	GAGATTAGACAGAGGAAAGAGTG
ITGAV_R	Reverse	AAGCAGACGACTTCAGAGAATAG
ITGAX_F	Forward	GCAGAATCAACCACCTCATCTTCCG
ITGAX_R	Reverse	CTCACATTGGCTGTCAGAAG
ITGB1_F	Forward	CTTGTCCAGAACTGAGTGAA
ITGB1_R	Reverse	GCTGACTTAGGGATCAAGTTT
ITGB2_F	Forward	GACCGCTACCTCATCTATGTGG
ITGB2_R	Reverse	GAATGCCGATCAGCACGATG
ITGB3_F	Forward	TCCATCCTGTATGTGGTAGAAG
ITGB3_R	Reverse	CAAGGCCAATGAGCAGAATG
ITGB4_F	Forward	AGGGCATCATCACCATAGAG
ITGB4_R	Reverse	GATGCTGCTGTACTCGCTTTG
ITGB5_F	Forward	GGGGAGATGTGTGAGAAGTGC
ITGB5_R	Reverse	GGTCTGGTTGTCAGGTTTCCC
ITGB6_F	Forward	ACCATCATTCACAGCATCAA
ITGB6_R	Reverse	GAGAAGAATAGCCAGGGAAAC
ITGB7_F	Forward	GTCGTGCTCAGAGTGAGACCC
ITGB7_R	Reverse	AGCCGGTAAGCCAGGACCAG
ITGB8_F	Forward	TCTCATGGAACAACAGCATTATG
ITGB8_R	Reverse	GACTTTAAGCAACCCAATCAAG

1159

1160

1161